

**Contractile properties of diaphragm muscle fibres isolated from rabbit containing the
R403Q mutation in heart**

© Anju Philip, 2016

A thesis submitted to McGill University in partial fulfilment of the requirements for the degree
of Master of Science

Department of Kinesiology and Physical Education

Faculty of Education

McGill University

Montreal, Quebec, Canada

December 2016

TABLE OF CONTENTS

ACKNOWLEDGEMENTS	iii
CONTRIBUTION OF AUTHORS	iv
LIST OF FIGURES	vi
ABSTRACT	viii
RÉSUMÉ	ix
CHAPTER I: LITERATURE REVIEW	1
INTRODUCTION	2
Hypertrophic cardiomyopathy (HCM).....	3
2.1 Genetic involvement.....	4
2.2 Clinical manifestation.....	4
Animal model used for study	5
3.1 R403Q mutation	6
3.2 Rationale for using rabbit model	7
Respiratory muscle weakness in cardiomyopathy.....	9
1.1 Evidence of diaphragm involvement in CHF and cardiomyopathy	10
1.2 Respiratory muscle weakness investigated through animal models.....	11
Muscle Contractile Properties	13
4.1 Force generation and relaxation rates.....	14
4.2 Force redevelopment following active shortening	17
4.3 Force enhancement during stretch.....	21
4.4 Passive forces and role of titin.....	23
Summary.....	24
CHAPTER II: EXPERIMENTAL ARTICLE	30
ABSTRACT	31
INTRODUCTION	32
METHODS	33
RESULTS	38
Isometric force:.....	38

Force enhancement during and after stretch of activated fibres:	39
Passive force - SL relation:.....	45
DISCUSSION	45
Comparisons with other studies:	46
Causes of impaired diaphragm muscle fibre contractility:	46
Limitations.....	48
Conclusion.....	48
CHAPTER III: CONCLUSION AND FUTURE DIRECTIONS	49
REFERENCES:	52

ACKNOWLEDGEMENTS

First and foremost, I would like to thank Dr Dilson Rassier, my supervisor, for giving me the opportunity to complete my master's degree in the Muscle Physiology and Biophysics Lab. He instilled in me a quest for knowledge and the need to focus on detail - skills that guided me throughout my duration of the study. He's always supported me, be it in the capacity of academic advisor for scientific understanding, or in the form of a mentor to adjust and accommodate to the non-academic environment. He has been a source of inspiration to me throughout my program – both as a teacher and a friend. I will be eternally grateful to him for his patience.

Secondly, I'd like to express my appreciation to Canadian Institute of Health Research (CIHR), the WYNG trust Foundation (WYNG trust Fellowship), Department of Kinesiology and physical education (Graduate excellence award) and the Education Graduate Students' Society (EGSS Master's student Leadership award) for their financial support.

Thirdly, I would like to thank Dr Fabio Minozzo and other members of the Muscle physiology and biophysics lab including Felipe Leite, Albert Kalganov, Nabil Shalabi, Yu-Shu Cheng and Giulia Del Guercio Green for their direct and indirect help in my research and for providing a positive work environment.

I would also like to thank my friends (Kiruthika, Anne-Catherine, Neha, Jocelyn, Karishma, Aravind, Sreekanth, Boopathy and Somnath) for their continuous support and for their companionship in Montreal. Lastly, I am grateful to my family and Allwin, who supported and encouraged me to pursue my goals.

CONTRIBUTION OF AUTHORS

Anju Philip was the primary author and played the principle role in experimental design and setup, data collection, data analysis, and thesis/manuscript preparation.

Dr Fabio Minozzo and Dr Felipe Leite contributed to data interpretation

Dr Dilson E. Rassier conceived the study; and contributed to data analysis and interpretation, and preparing the final draft of the thesis/manuscript

LIST OF FIGURES

- Figure 1:** Model of a sarcomere. Starting at the level of diaphragm right up to the level of a single sarcomere the figure depicts all the organisational levels within a muscle. adapted from Ottenheim et al
1 14
- Figure 2:** Schematic representation of molecular states during the crossbridge cycle. A – Actin, M – Myosin, ADP – Adenosine diphosphate, ATP – Adenosine triphosphate, P_i – Inorganic phosphate. Stage 1 – The powerstroke: P_i and ADP are released from the Actomyosin-ADP- P_i complex after completion of powerstroke. Stage 2 – myosin releases ADP, this releases the myosin from actin, the same free myosin rebinds to ATP to re-start powerstroke. Stage 3 – the myosin head weakly binds to actin, ATP on the myosin head hydrolyzes into ADP and P_i , and the energy released can be used for the powerstroke. .. 16
- Figure 3:** Biphasic time course of force relaxation initiated by sudden Ca^{2+} removal. The force decay has an initial slow, almost linear phase (slow k_{REL}). then a “shoulder” which is followed by a fast, nearly mono-exponential phase (fast k_{REL}). Adapted from Poggesi 2005⁴ 17
- Figure 4:** Equation fitted to force-velocity data derived from a single muscle fibre. Initially the first term in Hill’s equation was fitted by least squares method to data truncated at 0.78 P_0 , deriving numerical values for a and b. Thereafter, constants k_1 and k_2 were determined by fitting the equation to all the data points, including loads over 0.78 P_0 . Inset shows the shaded high-force portion of the graph in detail. Adapted from Edman 20
- Figure 5:** Slack test method: Superimposed data from a single muscle fibre showing three slack releases of different amplitudes during the plateau of tetanus contraction. Lower traces: release steps calibrated in μm (SL); and upper traces: tension recorded in the fibre. Adapted from Edman 20
- Figure 6:** Schematic representation of muscle force enhancement during stretch and residual force enhancement. Two superimposed contractions from the same muscle as it’s first activated, then stretched to a certain final length and finally relaxed (solid lines); and then activated isometrically and kept at the same final length before being relaxed again (dashed lines). Top panel: force traces. Bottom panel: length traces. P_c : critical force, FE: force enhancement during stretch, RFE: residual force enhancement and PFE: passive force enhancement. ‘a’ and ‘b’ represent the force transients during stretch. Adapted from Minozzo⁵ 22
- Figure 7:** Photographs of single muscle fibres of the diaphragm in the experimental chamber. A typical diaphragm fibre isolated from a wild type (WT) rabbit (A) and from the diaphragm of a R403Q rabbit (B). There is no visible difference in the striation pattern and structure of the fibre between the two groups. 34
- Figure 8:** Isometric contractions recorded during typical experiment with WT and R403Q diaphragm fibres. These traces are normalized to crosssectional area of the respective fibre. Note that the isometric force recorded for R403Q is lower than the WT. 39

Figure 9: (A) Rate of force redevelopment (k_{tr}). Typical force traces in experiments measuring k_{tr} in WT and R403Q muscle fibres. (B) Mean values k_{tr} recorded for both groups. Solid bars are the mean data recorded while the extended bars represent the standard error. Note that higher k_{tr} would suggest that R403Q redevelops force faster than the wild type, but there is no statistical difference in the k_{tr} (Mean \pm SE) of both the groups. 40

Figure 10: Typical force traces of single muscle fibres isolated from WT (1) and R403Q (2) rabbits, showing force enhancement during stretch (P_1 and P_2) and after stretch (FE 1 and FE 2). The isometric force and the peak force during the active stretch are lower in the R403Q fibre (P_2) when compared to the WT fibre (P_1). Force enhancement after stretch, calculated as the difference in force recorded after stretch and the isometric force produced during contraction, was lower for the rabbits with R403Q mutation (FE 2) relative to WT (FE 1) 41

Figure 11: (A) Mean values for force recorded during isometric contraction (Iso), point of maximal stretch (Peak) and force enhancement observed after stretch (FE). The force enhancement measured during and after stretch of activated fibre is significantly lower in diaphragm fibres extracted from R403Q when compared to WT ($P < 0.05$). (B) Mean unloaded shortening velocity. There is no statistical difference between unloaded shortening velocity (V_{max}) computed for the two groups (Mean \pm SE)... 42

Figure 12: Raw data traces showing experiments performed for evaluation of V_{max} in diaphragm muscle fibre extracted from WT and R403Q fibres. Four separate slack tests, corresponding to length steps of 5, 10, 15, 25% Lo, were performed on each fibre. The time required for the force to redevelop was plotted relative to the imposed length step. V_{max} was derived as the slope of the first order least squares regression line fitting the data. Inset: Zoomed view of the unloaded shortening velocity traces. 43

Figure 13:(A) Raw data traces for passive force – SL relation of WT and R403Q diaphragm muscle fibres. Consecutive stretches performed at pCa^{2+} 9.0 with individual fibres isolated from the diaphragm of WT and R403Q rabbits. The forces produced during and after stretches are the same for both the group. The bottom panel shows the step length ramp imposed on the fibres for this protocol. (B) Means (\pm SE) of Passive force - SL relation for all fibres investigated in this study. Both the peak forces during stretches (triangles – peaks) and the passive forces after stretches (circles – trough) were calculated to be similar between the groups. 44

ABSTRACT

Rationale: Respiratory muscle weakness is frequently reported as a secondary and independent predictor of mortality in patients with Familial Hypertrophic Cardiomyopathy (HCM). The mechanism of diaphragm weakness is not yet properly understood. In this study, we investigated the contractile properties of the diaphragm in a rabbit model with cardiac mutation (R403Q) that leads to HCM.

Objective: To test the hypothesis that diaphragm muscle fibres from R403Q rabbit model are weaker than wild-type (WT) littermates.

Hypothesis: i) R403Q diaphragm muscle fibres will produce lower isometric force; ii) the force drop will be due to changes in the crossbridge kinetics of the diseased diaphragm muscle.

Method: Five sets of experiments were performed on isolated skinned diaphragm muscle fibres of WT (n=21) and R403Q rabbits (n=17), to assess force development, force redevelopment following shortening, force enhancement during and after stretch, unloaded velocity and passive forces.

Results: R403Q fibres produced 39% lower force than WT fibres ($P < 0.05$). R403Q fibres also reported a drop of 21% and 34% in the forces produced during and after stretch respectively ($P < 0.05$). However, these fibres presented a similar kinetics of force redevelopment (k_{tr}) and unloaded shortening velocities (V_{max}). There was no difference in the passive force – sarcomere length (SL) relation between the two groups.

Conclusion: In accordance with our first hypothesis the diaphragm fibres from R403Q rabbits are weaker than WT. However, these alterations could not be explained by crossbridge kinetics alone but are likely the result of alterations in the structural composition of the muscle fibres.

RÉSUMÉ

Justification: La faiblesse des muscles respiratoires est citée comme prédicteur de mortalité secondaire mais indépendant chez les patients atteints de cardiomyopathie hypertrophique familiale (HCM). Pourtant, nous ne comprenons pas encore très bien le mécanisme de faiblesse du diaphragme. Dans cette étude, nous avons étudié les propriétés contractiles du diaphragme dans un modèle de lapin avec la mutation cardiaque (R403Q) menant à la HCM.

Objectif: Tester l'hypothèse selon laquelle les fibres musculaires de diaphragme du modèle de lapin R403Q sont plus faibles que celles de ses congénères de type sauvage (WT).

Hypothèses: i) Les fibres musculaires de diaphragme R403Q produiront une force isométrique inférieure; ii) la diminution de la force sera due aux altérations de cinétiques de pontages croisés du muscle de diaphragme malade.

Méthode: Cinq séries d'expériences ont été réalisées sur des fibres musculaires de diaphragme dépouillées et isolées, de lapins WT (n = 21) et R403Q (n = 17), afin d'évaluer le développement de la force; le redéveloppement de la force après raccourcissement; l'augmentation de la force pendant et après l'étirement; la vitesse sans charge; et les forces passives.

Résultats: Les fibres R403Q ont produit 39% moins de force que les fibres WT (P <0,05). Les fibres R403Q ont également marqué une baisse de 21% et de 34% des forces produites pendant et après l'étirement (P <0,05), respectivement. Cependant, ces fibres présentaient des cinétiques de redéveloppement de force (k_{tr}) et des vitesses de raccourcissement sans charge (V_{max}) similaires. De plus, la relation entre la force passive et la longueur de sarcomère (SL) était la même chez les deux groupes.

Conclusion: Conformément à notre première hypothèse, les fibres de diaphragme des lapins R403Q sont plus faibles que celles des WT. Cependant, ces différences n'ont pu être expliquées que par les cinétiques de pontages croisés, et sont probablement le résultat de modifications de la structure des fibres musculaires.

CHAPTER I:
LITERATURE REVIEW

INTRODUCTION

In mammals, the circulatory system and the respiratory system work in conjunction to oxygenate every part of the body. While the respiratory system extracts the oxygen with every breath by recruiting inspiratory muscles, the cardiac muscle pumps and delivers the oxygen to every cell in the body through the extensive network of the artery, veins, capillaries, and the lymphatics. The survival of the organism is dependent on the effective functioning of the cardiovascular system as a unit.

The presence of underlying cardiac anomalies, like cardiomyopathy, increases the load on the respiratory muscles^{6,7}. The heart, with its autonomous conduction system (the sinoatrial node, the atrioventricular node, the bundle of HIS, the right and left bundle branches, and the Purkinje Fibres), is usually apt to maintain its physiological functions despite a variety of pathological problems – genetic or acquired. Nevertheless, the increased strain on the respiratory system induces secondary changes in the neurophysiology of the respiratory musculature^{7,8}, which in turn leads to decreased quality of life.

Cardiomyopathies are diseases resulting from a wide array of conditions that damage the heart and other organs and result in cardiac dysfunction including infection, ischemia, congestive heart failure and sudden death. Studies of cardiomyopathic patients have demonstrated impaired skeletal muscle functions, especially the diaphragm, including muscle atrophy and changes in muscle fibre type composition^{6,9-11}. With the advancement of genetics, animal models of cardiomyopathy have emerged as important research tools to study pathophysiology, progression, and treatment of respiratory muscle dysfunction in congestive heart failures, one of the major clinical findings in cardiomyopathy¹²⁻¹⁶.

The majority of research on cardiomyopathy indicates that impaired cardiac function may not be the only determinant of respiratory muscle weakness and associated exercise intolerance and dyspnea with cardiomyopathy^{10,17-22}. Most of the literature on respiratory muscle adaptations in cardiomyopathy are conducted on murine models that manifest two or three of the symptoms clinically reported in patients with cardiomyopathy; cardiac hypertrophy, myocyte disarray, interstitial fibrosis, ventricular arrhythmias, sudden death or phenotype heterogeneity²³. However, the nature of the respiratory adaptive response to congestive heart failure remains controversial, with some mutations reporting increased force generation in diaphragm muscle²⁴⁻²⁶ thereby indicating a positive adaptation to the disease, while others indicate a decrease in function.

In order to understand the effects of cardiomyopathy in the respiratory muscles, it is imperative to select a mutation and animal model that appropriately recapitulates the phenotypes manifested in human cardiomyopathies. Studies in the appropriate animal models will provide a better understanding of the pathophysiology and mechanisms of respiratory muscle impairment in cardiomyopathy, and thereby help develop targeted therapeutic approaches.

Hypertrophic cardiomyopathy (HCM)

Traditionally, cardiomyopathies are classified according to morphological and functional criteria: dilated cardiomyopathy, hypertrophic cardiomyopathy, restrictive cardiomyopathy, and arrhythmogenic right ventricular cardiomyopathy²⁷. Hypertrophic cardiomyopathy (HCM) occurs once in every 500 births and is the most common inherited heart disease²⁸, with diverse genetic and phenotypic expression, clinical presentation and natural disease progression. It affects all races, both sexes, on all continents²⁹. HCM is now recognised as the most common cause of sudden cardiac death in athletes as well as in adolescents but may present at any age. The European

society of cardiology defines HCM as a disease marked by increased left ventricular (LV) wall thickness that is not solely explained by abnormal loading conditions³⁰. Clinically the disease is characterised by the asymmetric left and/or right ventricular hypertrophy, usually involving the interventricular septum²⁸.

2.1 Genetic involvement

In 60% of those affected the disease had an autosomal dominant trait caused by mutations in any one of 10 genes, each gene encoding cardiac sarcomere protein. Predominantly, mutations in the encoding beta-myosin heavy chain (β -MHC) cardiac troponin T and myosin-binding protein C, less commonly seen mutations affecting the cardiac troponin I, alpha tropomyosin chain, regulatory and essential myosin light chains, titin, alpha-actin and alpha myosin heavy chain (α -MHC) have also been reported. Individuals with multiple sarcomeric protein mutations (up to 5%) present with a more severe phenotype than those without a mutation³⁰. The vast heterogeneity within the genes itself and missense of over 150 mutations identified compounds the diversity of the clinical manifestations observed in HCM patients²⁸. Thereby establishing that genetic involvement which predisposed an individual to HCM.

2.2 Clinical manifestation

One of the important clinical manifestations of HCM is the presence of undilated left ventricular (LV) hypertrophy. HCM may be detected early in the presence of a cardiac murmur, abnormal electrocardiographic recordings, and a positive family history. The onset and diagnosis of HCM are dependent on the severity and type of the gene mutations. In individuals with HCM due to cardiac myosin binding protein C or troponin T mutations, the onset of LV hypertrophy may occur as late as midlife or even later. Also, a small subset of HCM patients may survive into

the end stage ('burned-out' phase), which is characterised by LV wall thinning, cavity enlargement, and even systolic dysfunction. LV hypertrophy can appear at any age and also increase or decrease dynamically throughout life, thereby establishing that HCM is not a static disease ²⁸.

Histologically, the autopsies obtained from patients show chaotically arranged intercellular connections of hypertrophied cardiac muscle cells. This cellular disarray is widely distributed, mostly in portions of LV wall and is more extensive in young patients. The presence of abnormally thickened coronary artery with increased collagen and narrow lumen adds to the cardiovascular structural architecture, leading to impaired coronary circulation and bursts of myocardial ischemia. Ischemia-induced death and repair of myocyte results in myocardial scarring, frequently seen within the natural history of HCM. The cardiac disarray, myocardial scarring, and the expanded interstitial matrix collagen contribute towards impaired diastolic function as well as arrhythmogenic substrates. The severity and progression of this complex disorder depend on the nature of the mutation itself. In some cases, patient present no symptoms, but sudden death is caused by HCM ^{28,30-32}.

Animal model used for study

HCM is a complex and heterogeneous cardiovascular disorder both genetically as well as in its clinical manifestations. 70% of patients genotyped successfully have mutations in two genes, β -myosin heavy chain (β -MHC) and myosin binding protein C. Troponin T and several other genes account for 5% or less, respectively ²⁹. Over 1400 mutations, mostly missense, have been identified over the years; most of these mutations are unique to the individual families ³¹. Though α -myosin heavy chain (α -MHC) and titin have also been linked with HCM their pathogenicity reported is

not that severe ²⁸. Major advances in technology have resulted in clinical characterization and identification of causative gene mutations in patients with HCM. Many questions regarding the underlying disease mutation remain unanswered. Animal models of HCM have been developed to gain insight into the disease pathogenesis, mechanism, progression of the disease and therapies.

3.1 R403Q mutation

β -MHC mutations account for 30 - 35% of all gene defects in HCM families ³². β -MHC is the major contractile protein of the thick sarcomeric filament, responsible for normal cardiac contractions. The predominance of MHC isoform (α - or β -) in the heart ventricles varies between species. While α -MHC isoform predominates in mice, β isoform is most prevalent in humans and rabbits ³³.

The missense mutation of arginine to glutamine at amino acid 403 (R403Q) in the β -myosin heavy chain (MHC) was the first mutation identified to cause HCM ³⁴. It is also the most extensively studied of all HCM mutations. R403Q mutation has high penetrance; more than 90% individuals carrying the gene express cardiomyopathic phenotype within the first 20 years of birth. Almost 50% of affected individuals succumb to sudden death by the age of 45 years ³⁵.

The first HCM animal model engineered genetically reproduced the R403Q mutation in mice ³⁶ and it provided consolidated evidence that sarcomeric gene mutations lead to HCM. It was created by introducing the R403Q mutation into one of the endogenous alleles of mouse cardiac α -MHC gene. The heterozygous model (α -MHC403/+) recapitulated the phenotype of the human disease – mice developing diastolic dysfunction, myocyte hypertrophy, cardiac disarray and interstitial fibrosis. Early onset of disease, with left ventricular hypertrophy that was evident by 30

weeks; however, the disease severity was age-dependent, and the cardiac systolic dysfunction and histopathology worsening with age^{37,38}.

3.2 Rationale for using rabbit model

Most the existing literature about R403Q induced HCM is based on rodent models. Rodents are relatively inexpensive and their short gestation period allows researchers to produce a large sample size over a shorter period. However, a major concern with studies on a murine model for human HCM caused by β -MHC lies in the cardiac sarcomeric composition. β -MHC protein is the predominant protein in the ventricle of humans comprising greater than 95% of the total myosin pools, and the murine cardiac ventricle is predominantly α -MHC, and the β -MHC protein is expressed as less than 5% of the total cardiac myosin content³⁹. The major difference between α - and β -MHC lies in the actin-activated Mg-ATPase activity and crossbridge cycling rates, with ATPase activity being highest for α -MHC and lowest for β -MHC. The duration of force-transients in the α -MHC is shorter than in the β -MHC. Physiologically, the mouse heart beats 10 times faster than the human heart, which in turn influences the refractory period associated with arrhythmia.

Since α - and β - myosin isoforms have 93% similarities in amino acid sequencing, it has been assumed that the different backbones would have little functional consequences. Lowey et al. developed a transgenic mouse model in which the endogenous α -MHC was replaced with β -MHC to compare the functional properties of R403Q expressed in β -cardiac MHC with that of the α -cardiac MHC⁴⁰. The study reported a 30-40% increase in actin filament velocity in the in-vitro motility assay of R403Q α -MHC mice compared with wild type. However, there was no enhancement in velocity in R403Q β -MHC mutant mice. They also found that the actin-activated MgATPase activity was 30% higher in R403Q α -MHC than for wild type, whereas the enzymatic

activity was reduced by 10% in β -MHC. In 2013, Lowey et al. used stopped-flow kinetics to understand the mechanochemical properties of the myosin mutation in both the isoform backbones⁴¹. They employed stopped flow kinetics to measure the rate of ADP release from the myosin heads and the equilibrium constants. They observed that with the R403Q mutation at the actomyosin interface, the α -myosin head released almost 20% more ADP release, whereas the same mutation resulted in reduced ADP release in mice with the β -myosin head unit - the affinity of MgADP for α -MHC subunit is almost 4-fold weaker than for β -MHC. These studies established that the functional effects of R403Q mutation are dependent on the type of MHC isoform affected.

The advantage of the rabbit model over the mice model is that the rabbit ventricle is predominantly made of β -MHC (greater than 85% of total myosin). Also, the similarities in heart rates and cardiac size make rabbit models ideal for physiological studies. Marian et. al. developed a transgenic rabbit model for HCM by introducing a point mutation in the β -myosin heavy chain (MHC) gene, R400Q⁴². Wild-type (R⁴⁰³) and the mutant human β -MHC (Q⁴⁰³) complementary DNAs were first cloned 3' to a 7-kb murine β -MHC promoter. These purified transgenes were then injected into fertilised zygotes of donor rabbits, to generate two lines each of the wild-type and mutant transgenic rabbits. Northern blotting and 2-dimensional gel electrophoresis followed by immunoblotting of the cardiac tissues confirmed the expression of transgene mRNA and protein, respectively. Rabbits carrying the mutant transgene showed significant myocyte disarray, interstitial collagen expression in their myocardium was reported to be raised to three times in comparison with transgenic wild-type and nontransgenic littermates (NLMs) increased up to three times. The mean septal thickness of the transgenic mutant was significantly being greater than that recorded for transgenic wild-type rabbits and the NLMs, which were comparable. Similarly, the posterior wall thickness and left ventricular mass were also increased in the mutant transgenic

rabbit relative to transgenic wild-type and NLMs. However, the overall cardiac dimensions including left ventricular end diastolic diameter and end systolic diameter were similar across all the three groups of rabbits. Premature death was more common in mutant transgenic rabbit than in wild-type transgenic rabbits or in NLMs. This high incidence of premature death in the mutant rabbit is in accord with a high incidence of sudden cardiac death associated in cardiomyopathic patients with the R403Q mutation. All these findings are consistent with the clinical symptoms of patients with HCM with R403Q mutation, thereby establishing that the R403Q transgenic rabbit model is appropriate to study the pathogenesis of human HCM.

Respiratory muscle weakness in cardiomyopathy

Congestive heart failure (CHF) is one of the most common causes of mortality in patients with cardiomyopathy. Patients with CHF frequently complain of breathlessness and shortness of breath even with mild exercise and this affects their quality of life ^{7,43}. The diaphragm is the primary inspiratory muscle of the respiratory system and a decrease in its efficiency is probably due to the reduction in the compliance, increase in airflow resistance and decrease in diffusing capacity of the respiratory system ⁴⁴. The presence of an alteration in respiratory muscle perfusion ⁴⁵ and increased ventilator load ²² indicates diaphragm muscle weakness, which contributes to breathlessness and respiratory limitation reported in patients with CHF ⁴⁶. There are evidence of sarcolemmal damage and sarcomeric loading resulting from an increase in diaphragmatic workload ^{47,48}. Additionally, diaphragm muscle biopsies of patients with CHF show fibre type redistribution from fast to slow oxidative fibres ^{25,49}. It has been established that maximal inspiratory pressure is reduced in CHF patients, and respiratory muscle strength may serve as an independent predictor of disease progression and prognosis after treatment for CHF ⁵⁰.

1.1 Evidence of diaphragm involvement in CHF and cardiomyopathy

Müller-Höcker et.al. reported the presence of mitochondrial myopathy in the diaphragm of a 5-month old boy who succumbed to cardiomyopathy ⁵¹, in 1991. The child reported respiratory arrest and seizures as early as 3 days after birth and 3 months later acquired upper respiratory tract infection, which progressed to dyspnea. He required continuous respiratory ventilation until he died of irreversible cardiac arrest. An autopsy of the heart revealed the absence of necrosis and cellular disarray of cardiomyocyte, commonly associated with cardiomyopathy. However, the heart showed marked biventricular hypertrophy, the cardiac muscle cells had accumulations of enlarged mitochondria and the myofibril content was reduced. Accumulation of lipid droplets and abnormal mitochondria led to a loosening of the myofibrils in the diaphragm muscles especially those with structural abnormalities. Additionally, cytochrome c oxidase staining and ultra cytochemistry revealed that both the heart and diaphragm myocytes had portions of muscles devoid of enzyme activity and deficient mitochondrial activity.

Evaluation of 47 cardiomyopathy patients with chronic heart failure revealed a reduction in lung volumes and diffusion capacity in comparison to healthy subjects ⁵². A reduction in respiratory muscle strength was observed in patients with cardiomyopathy and it was more pronounced in those with severe chronic heart failure leading to slight changes in breathing patterns.

One and two-dimensional electrophoretic techniques were used to investigate myofibrillar protein composition in human diaphragm samples obtained from biopsies of 10 CHF patients and 7 control subjects ⁴⁹. The percentage of slow MHC I was increased from 43%, observed in control subjects to 57% in patients with CHF, while the fast MHC IIb was decreased to 8% from 17%. A

similar trend was observed in myosin light chain (MLC) composition with an increase in all slow MLC isoforms and a decrease in all fast MLC isoforms. Diaphragm from CHF reported a consistent drop in percentages of fast isoforms of Troponin-T and Troponin-I and an increase in Troponin-C.

These results reveal that CHF induces a fast-to-slow transformation in myosin as well as other muscle regulatory proteins. Another study by Tikunov²⁵ investigated diaphragmatic biopsies from 10 patients with cardiomyopathy-induced heart failure and 7 brain-dead organ donors served as control subjects. The study established a fast to slow MHC isoforms shift in the diaphragm in conjunction with an increase in oxidative capacity and a drop in glycolytic capacity. These results are like those elicited during endurance training of the limb muscles in normal subjects.

1.2 Respiratory muscle weakness investigated through animal models

In 1998, Lecarpentier & Coirault⁵³, used rabbit diaphragm muscle strips to investigate for the first time the myosin-actin crossbridge properties of the inspiratory muscle in congestive heart failure. Combined volume and pressure overload were used to induce CHF in 9 rabbits, while 14 sham-operated rabbits were used as controls. They reported a decrease in the total number of crossbridges attached to actin and a significant drop in the force produced by individual crossbridges. The drop in peak mechanical efficiency of CHF diaphragm in addition to marked changes in crossbridge kinetics added to the disadvantageous energetic conditions of CHF diaphragm, resulting in impairment of diaphragmatic performance in the CHF rabbit model. De Souza et. al. investigated the diaphragm of CHF rats⁸, and reported a marked increase in type I and type IIa MHC, thereby establishing an adaptive transformation towards a slow and more economic contraction to compensate for the increased workload. However, the maximal oxidative

capacity of the permeabilized fibres was considerably reduced in CHF diaphragm, suggesting a disease-induced alteration in mitochondrial function.

In order to understand the pathophysiology of CHF induced diaphragm weakness, Van Hees evaluated single muscle fibres of all the MHC isoforms present in diaphragm ²⁶. The study reported a decrease in maximal force generation and a relative loss in myosin heavy chain content across all single fibre type – slow, 2a, 2x. Additionally, the rate of force redevelopment of diaphragm single muscle fibres and calcium (Ca^{2+}) sensitivity of the fibre were substantially reduced. Increased activation of ubiquitin-proteasome pathway and its upstream proteolytic enzyme caspase-3 was suggested to be associated with the decrease diaphragm strength and loss of myosin heavy content. Another study by Study by Van Hees ⁵⁴ on CHF rats, demonstrated a reduction in isometric force and shortening velocity of diaphragm bundles from CHF rats together with structural abnormalities. The study also implied that the diaphragm muscles have decreased calcium sensitivity in CHF rats. In addition to myosin loss presence of swollen, degenerating mitochondria coincided with impaired contractility in the CHF diaphragm.

Lecarpentier examined the load dependence of relaxation in 15 rabbits with artificially induced CHF and compared them with 12 sham-operated control rabbits ²². In-vitro analysis of isolated muscles strips revealed a drop in isotonic as well as isometric relaxation in the diaphragm of CHF rabbits. A cumulative chronic volume and pressure overload resulted in high degree of cardiac hypertrophy and heart failure. The CHF diaphragm showed a marked reduction in load dependence of relaxation (almost 50%), The fall in LD of relaxation observed in CHF diaphragm paralleled that in contractile performance and suggests an abnormality in the sarcoplasmic reticulum.

Most of the studies have reported a loss in diaphragm muscle strength and a decrease in force generation in the diaphragm of animals with CHF^{21,23,26,43,52,53,55-59}. Additionally, it is well established that there is fibre type shift from fast to slow myosin isoform in the diaphragm of individuals suffering from cardiomyopathy induced chronic CHF^{6,25,49,60}. These adaptive fibre type transformations in diaphragm muscle in response to increased loading conditions are similar to muscle adaptations in endurance training and are contrary to recordings of lower force production. A recent study in our lab reported an increased force production by diaphragm myofibrils in a knockout mouse (KO) model with cardiac-specific deletion of arginyl-tRNA transferase, which induces cardiomyopathy and symptoms of congestive heart failure²⁴. The myofibrils from the myocardium of the KO mouse reported a reduction in active and passive forces at different sarcomere lengths (SL) but there were no associated changes in rates of force development, force redevelopment and relaxation in comparison with wild-type myocardium, suggesting that the changes in force observed are not due alterations in crossbridge kinetics. Interestingly, the increase in active force production in the diaphragm myofibrils of KO mice (despite a reduction in myofibrils per muscle fibre) suggests an increased load and drop in the number of myofibrils available which induces augmentative adaptation in the molecular mechanisms of force production.

Muscle Contractile Properties

Muscles are the basic locomotor units of all vertebrate, where the force produced is used to move bones and joints just like the system of levers and pulleys. As shown in Figure 1, muscles are made of tubular muscle fibres or myocytes, which in turn are made up of rod-like myofibrils. Myofibril contains series of contractile units called sarcomere made of myofilaments

actin and myosin proteins responsible for muscle contraction. Muscle generate force during isometric contractions, or during active shortening or lengthening.

Diaphragm muscle contraction, like other striated muscles, is regulated through the interaction of calcium (Ca^{2+}) with the thin filament, composed of actin, tropomyosin, and troponin, within every single sarcomere.

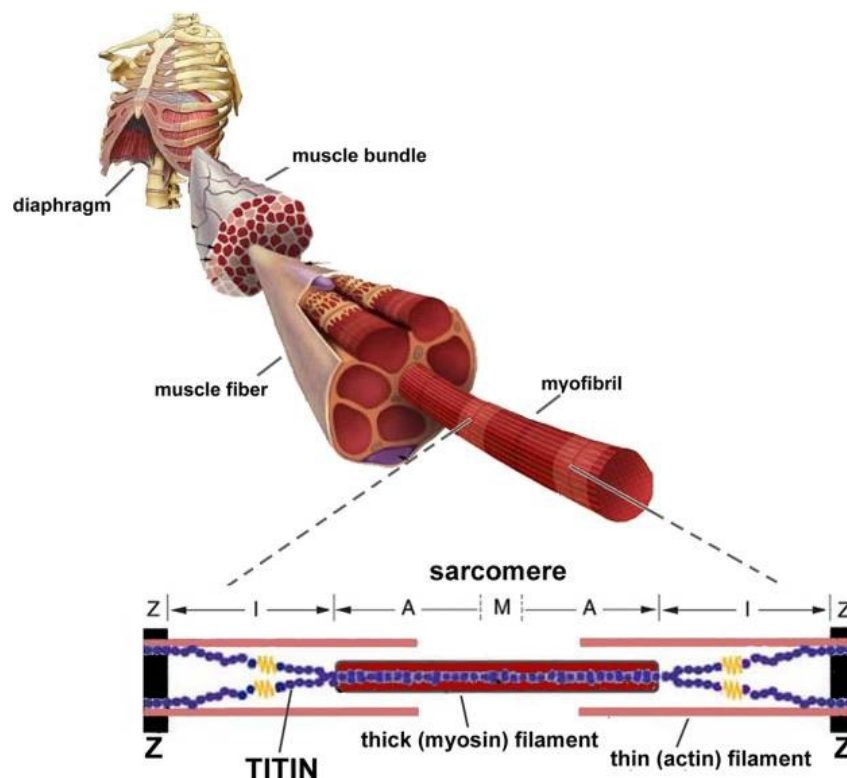


Figure 1: Model of a sarcomere. Starting at the level of diaphragm right up to the level of a single sarcomere the figure depicts all the organisational levels within a muscle. adapted from Ottenheim et al ¹

4.1 Force generation and relaxation rates

The “crossbridge model” of Huxley and Simmons ⁶¹ is the best predictor of the force development upon muscle contraction. Huxley postulated that crossbridges are formed between myosin and actin filaments in the presence of ATP, which drive these myofilaments to slide past

each other causing the muscle to contract. Subsequent models have been proposed supporting or complementing the crossbridge theory ⁶²⁻⁶⁴. In short, the crossbridge model suggests three molecular states: 1) Pre-powerstroke – a crossbridge formed by weakly bound myosin-actin interaction; 2) post-powerstroke state – a crossbridge formed by strongly attached myosin-actin interaction; and 3) a detached state – with no myosin-actin interactions or crossbridges.

The myosin head has been compared to a lever arm driven by actin binding and release of adenosine diphosphate (ADP) and inorganic phosphate (P_i). The “lever arm hypothesis” suggests that the release of ADP and P_i causes myosin head to swing and generate force. The attachment of ATP releases the myosin head from actin and forms the detached state. The hydrolysis of ATP induces the pre-powerstroke state, and the crossbridge cycle can repeat ^{65,66}.

In addition, there is a relationship between the force produced by the muscle and the length of the sarcomere ⁶⁷ - the amount of myosin-actin overlap predicts the amount of force of contraction. This force-length relationship is a function of the number of attached crossbridges ^{68,69}.

Skeletal muscle fibre relaxation is governed by Ca^{2+} transport proteins and sarcomere proteins. Experiments with intact muscle preparations have established that fall in calcium ion [Ca^{2+}] precedes relaxation and is considerably faster than force decay. Fall Ca^{2+} is not the sole determinant of relaxation rate (k_{REL}). Crossbridge mechanics and kinetics are major determinants of time course and “load-dependent” changes in relaxation kinetics.

The time course of relaxation following Ca^{2+} removal is biphasic. During the slow phase of relaxation, initiated by a reduction in calcium, sarcomeres can be maintained isometric for the whole transient. Poggesi et. al confirmed that even in the absence of Ca^{2+} , relaxation is achieved

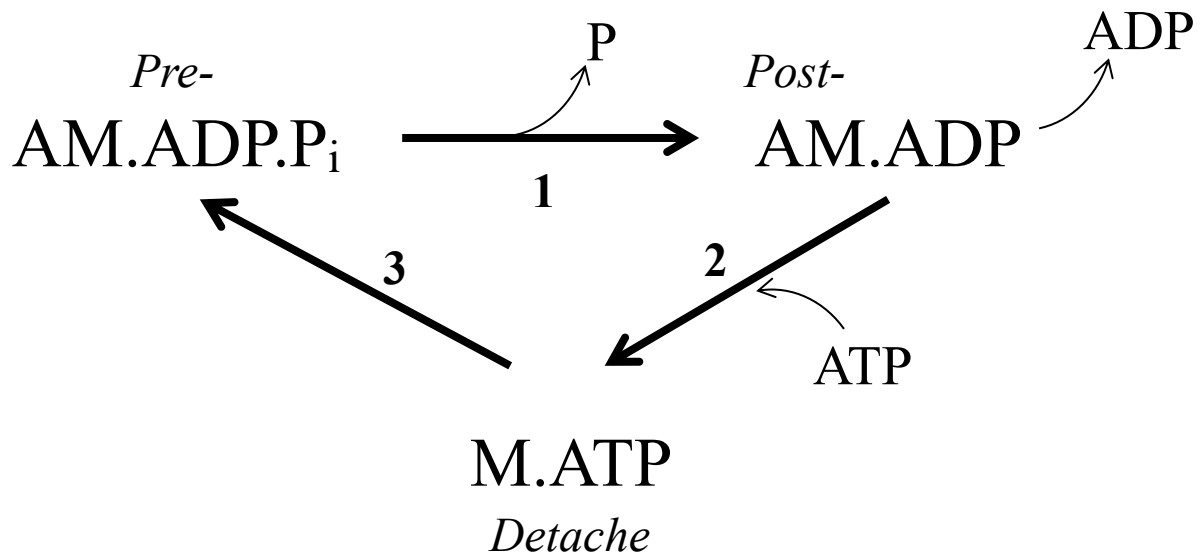


Figure 2: Schematic representation of molecular states during the crossbridge cycle. A – Actin, M – Myosin, ADP – Adenosine diphosphate, ATP – Adenosine triphosphate, P_i – Inorganic phosphate. Stage 1 – The powerstroke: P_i and ADP are released from the Actomyosin-ADP- P_i complex after completion of powerstroke. Stage 2 – myosin releases ADP, this releases the myosin from actin, the same free myosin rebinds to ATP to re-start powerstroke. Stage 3 – the myosin head weakly binds to actin, ATP on the myosin head hydrolyzes into ADP and P_i , and the energy released can be used for the powerstroke.

by blocking crossbridges from entering force-generating states, while the crossbridges that are currently in the force generating states decay away, even in the absence of Ca^{2+} .

Rapid elongation or “give” in some sarcomeres marks the transition between the slow and fast phase of force decay, also called the tension shoulder. At this stage, the average strain of force-

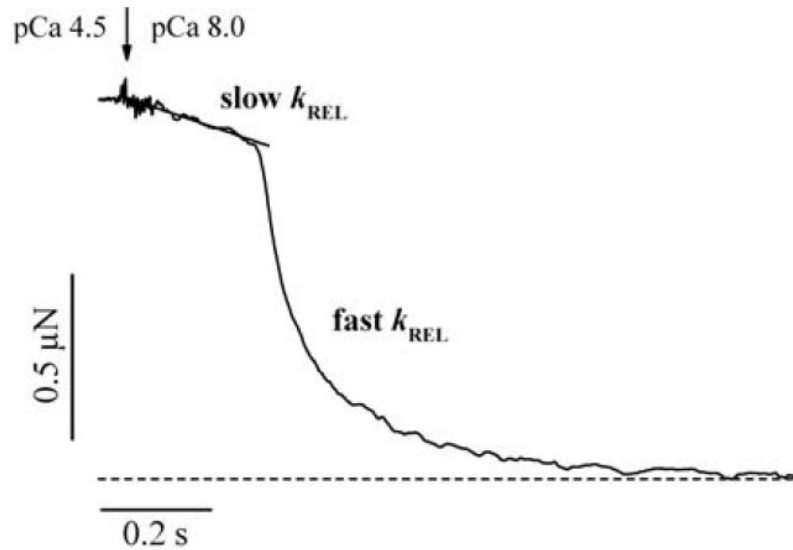


Figure 3: Biphasic time course of force relaxation initiated by sudden Ca^{2+} removal. The force decay has an initial slow, almost linear phase (slow k_{REL}), then a “shoulder” which is followed by a fast, nearly mono-exponential phase (fast k_{REL}). Adapted from Poggesi 2005 ⁴

generating crossbridges escalates the force beyond the threshold, which favours rapid crossbridge detachment and “give” of the weakest sarcomeres. Sequential propagation of sarcomere “give” from one sarcomere to the next continues even after force becomes negligible, all sarcomeres relax.

4.2 Force redevelopment following active shortening

Studies have investigated crossbridge kinetics using a force redevelopment protocol. In this technique, skinned muscle fibre producing a steady-state isometric force is allowed to shorten under unloaded conditions for a brief period, and shortly after it is re-stretched to its original length. This rapid shortening and re-stretching detaches most of the strongly bound crossbridges. The time course over which the crossbridges re-establish the force-generating capacity is a measure of the kinetics of crossbridge cycling and force-bearing states ⁷⁰.

4.2.1 Rate of force redevelopment (k_{tr})

Studies on force redevelopment in skinned muscle fibres have led to the development of estimation techniques for rate constant of crossbridge reattachment and force generation. The rate of force redevelopment (k_{tr}) after rapid release and restretch in skinned fibres helps one access the properties of the myosin at maximal Ca^{2+} activation^{70,71}. The rate constant for force redevelopment is estimated from the time to half-maximum redeveloped force. This rapid activation is primarily dependent on $[\text{Ca}^{2+}]$ and independent of the initial level of force. This is consistent with conclusions from the k_{tr} measurements that the activation rate results primarily from the kinetics of Ca^{2+} binding and the subsequent conformational changes of the thin filament.

4.2.2 The Force-velocity relationship and the maximum velocity of shortening.

The muscle adjusts its force to precisely match the load that it experiences during shortening by continuously adjusting the speed at which it moves. For a small load, the speed of shortening of contraction is fast, accounting for the lower force⁷². Conversely, for heavier loads the shortening velocity is lowered to produce higher active force. Hill suggested this inverse relationship between load and velocity as a primary property of muscle contraction⁷³.

The maximum speed of shortening attained when a muscle is free to shorten at zero loads represents the maximum cycling rate of the myosin crossbridges. Studies by Barany⁷⁴ and later by Edman et. al³ found that V_{\max} correlated well with the maximum rate of ATP splitting in whole muscle as well as in single fibre level, respectively.

Edman et. al³ conducted detailed studies on single muscle fibres to reveal that the force-velocity relationship manifests two separate curvatures, with an upward concavity on either side

of a breakpoint near 80% of the isometric force ($0.8 P_0$). The following empirical equation provides an excellent fit to the biphasic experimental data shown in figure 4:

$$V = \frac{(P_0^* - P)b}{P + a} \left(1 - \frac{1}{1 + e^{-k_1(P - k_2 P_0)}} \right)$$

where V represents the velocity of shortening, P is the load on the muscle fibre, P_0 denotes the measured isometric force. Constants a and b have dimensions of force and velocity, respectively; constant k_1 -has dimension of 1/force and determines the steepness of the high-force curvature; and constant k_2 , which is the relative force at which the correction term reaches its half value, is dimensionless. The first term represents the force-velocity relation below $0.8 P_0$ and the second term also referred to as ‘correction term’ reduces the V at higher loads for a better fit at loads greater than $0.8 P_0$. Constants k_1 and k_2 are used when computing V_{\max} .

Edman’s model ⁷⁵ proposes that there’s a Gaussian position-dependence of the attachment rate constant along actin, which provides a region for slow crossbridge attachment during early powerstroke. This explains the marked decrease in the number of crossbridges pulling during contraction in higher force range and a lower force output per bridge. It has been established that in contrast to muscle fibre’s ability to produce force, it’s maximum speed of shortening does not depend on the number of myosin bridges that are able to bind with the thin filaments ⁷², so V_{\max} is independent of the degree of activation of the contractile system.

One of the most convenient methods for measuring the speed of shortening at zero loads described by Edman ² is the slack test method. The muscle fibre is quickly released during mid-contraction thereby causing a rapid slack in the fibre, which leads to an abrupt fall in tension to

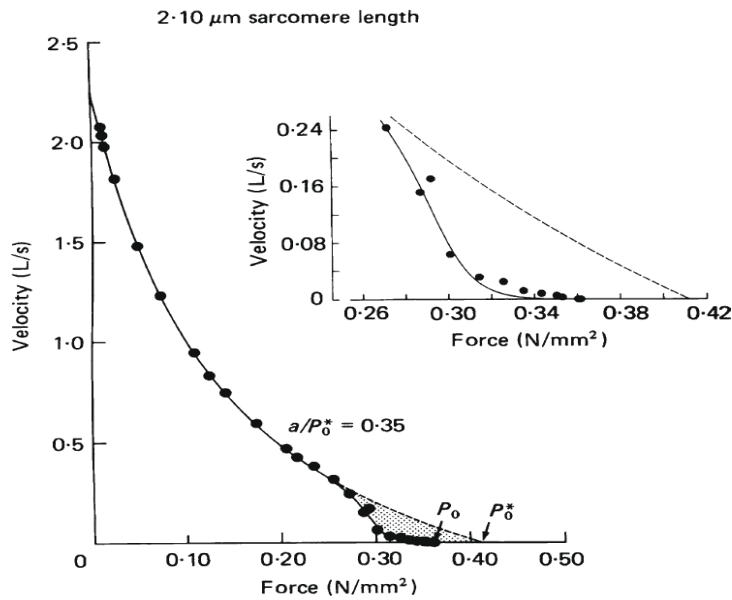


Figure 4: Equation fitted to force-velocity data derived from a single muscle fibre. Initially the first term in Hill's equation was fitted by least squares method to data truncated at $0.78 P_0$, deriving numerical values for a and b . Thereafter, constants k_1 and k_2 were determined by fitting the equation to all the data points, including loads over $0.78 P_0$. Inset shows the shaded high-force portion of the graph in detail. Adapted from Edman ³

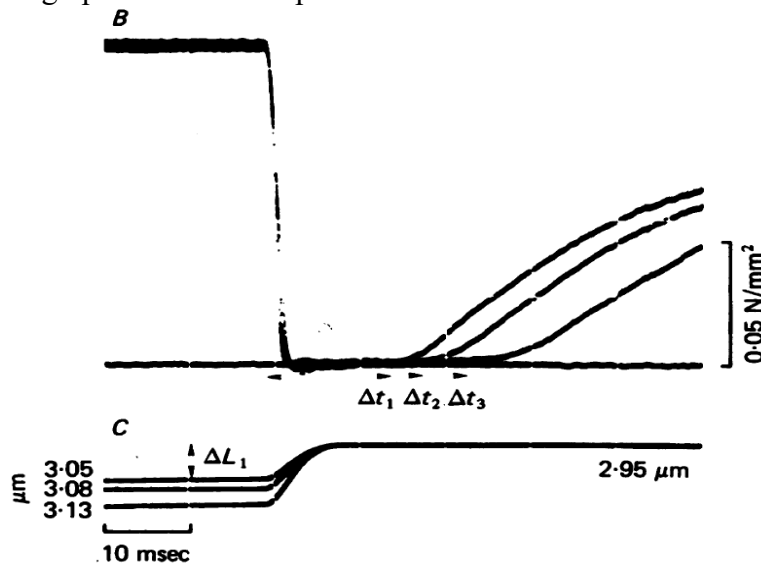


Figure 5: Slack test method: Superimposed data from a single muscle fibre showing three slack releases of different amplitudes during the plateau of tetanus contraction. Lower traces: release steps calibrated in μm (SL); and upper traces: tension recorded in the fibre. Adapted from Edman ²

zero. This allows the fibre to shorten actively to take up the slack. Three or more amplitudes of release (ΔL) are used. The lowest the time (Δt) measured from slack to the onset of force redevelopment is plotted against the release amplitude, and the slope of the straight line so obtained (regression analysis) provides a measure of the shortening velocity at zero load.

4.3 Force enhancement during stretch

If a muscle fibre is stretched while activated, there is a notable increase in force without a concomitant increase in ATP utilisation⁷⁶⁻⁷⁹, a phenomenon known as force enhancement during stretch. The force rises in two phases following a ramped stretch protocol (Figure 6). The critical force (P_c) (transition between these two phases) is associated with the force at which the attached crossbridges reach their maximum extension, at a critical SL, before detaching from actin⁸⁰. The increase in force during a stretch of activated fibre is associated with the pre-powerstroke crossbridges. Since these crossbridges are less strained than crossbridges in powerstroke, they would not contribute towards isometric force production. Instead, they would resist stretch leading to an increase in force during lengthening⁸¹⁻⁸⁴ with static tension (non-crossbridge force), mechanism independent of the crossbridges.

When a muscle fibre is actively stretched, there is an increase in force production explained by the strain developed by the crossbridges attached to actin during an active contraction⁸⁵. The steady-state force achieved is greater than the isometric force at corresponding length, also known as the **residual force enhancement**^{83,85,86}. The increase in force during active stretching is dependent on the speed of the muscle stretch, but the steady state force enhancement achieved is dependent on the magnitude of the stretch^{83,87-89}.

Residual force enhancement is long lasting and happens at longer SLs along the descending limb of the length-tension relation ^{78,83,90}. The mechanism behind the steady state force enhancement remains unclear, but the three main theories proposed are: 1) SL non-uniformities ^{91,92}, which postulates that force developed by one-half of the sarcomere is different from the force developed in the other half ^{89,93-96}; 2) an increase in the number and force produced by crossbridges in the contractile unit of the striated muscles ^{80,97-99}; and 3) increase in stiffness and passive force arising from involvement of titin molecule. ^{80,91,99-101}.

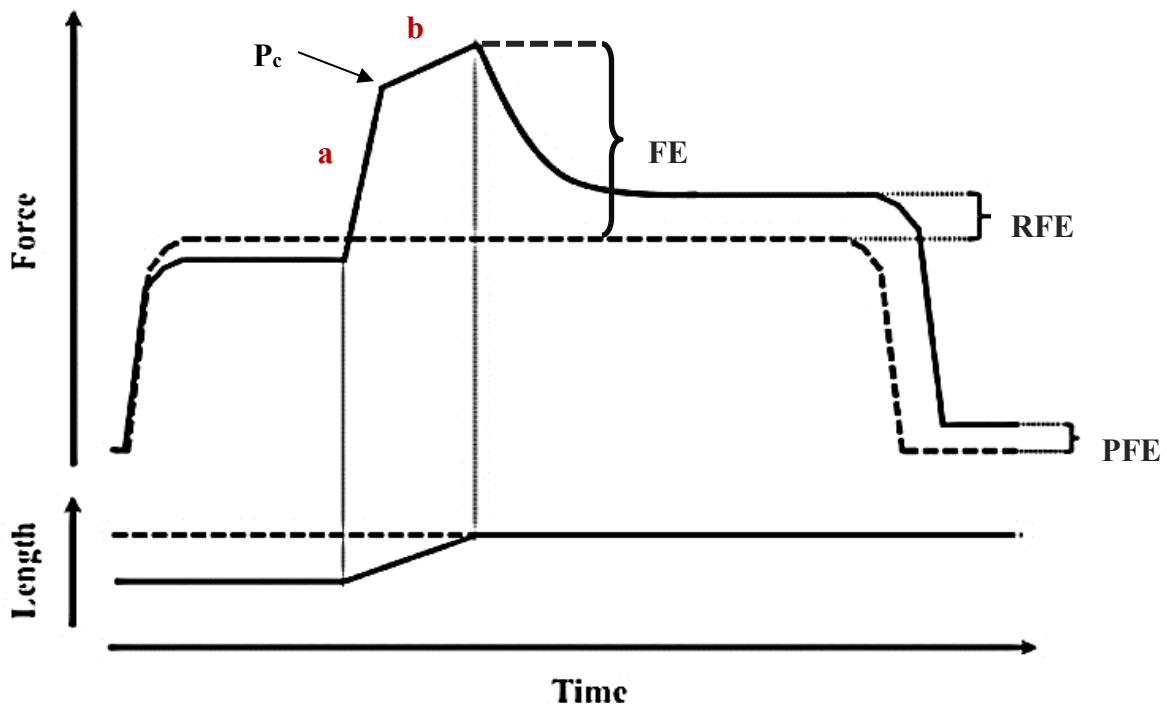


Figure 6: Schematic representation of muscle force enhancement during stretch and residual force enhancement. Two superimposed contractions from the same muscle as it's first activated, then stretched to a certain final length and finally relaxed (solid lines); and then activated isometrically and kept at the same final length before being relaxed again (dashed lines). Top panel: force traces. Bottom panel: length traces. P_c : critical force, FE: force enhancement during stretch, RFE: residual force enhancement and PFE: passive force enhancement. 'a' and 'b' represent the force transients during stretch. Adapted from Minozzo ⁵

4.4 *Passive forces and role of titin*

When a muscle fibre is stretched passively without being activated (i.e. not being stimulated to contract) there is an increase in force that is independent of the crossbridges. Studies have found the passive elastic component within the muscle is regulated by the elastic protein titin^{85,102-104}. Titin, the largest protein in the muscle, provides structural integrity and noncontractile force production. As a structural protein, it spans half the length of the sarcomere and maintains the myosin alignment over a dynamic range of SLs in striated muscles⁸⁵. Titin molecule has a spring-like characteristic that produces passive resistance in response to stretch¹⁰³. At high SLs where crossbridge interaction is not possible, titin is the primary contributor of noncontractile muscle force⁹⁰. The importance of titin to passive tension in the muscle is evident in developmental and disease states, where changes in titin isoforms lead to consequential changes in muscle elastic properties¹⁰⁵⁻¹⁰⁹. Because of its dynamic function in muscle physiology and pathophysiology, several recent studies have attempted to elucidate titin's role in the regulation of noncontractile force.

Most of titin's mass is made up of immunoglobulin domains and PEVK (proline, glutamine, valine, and lysine-rich) segment repeats derived from differential splicing of isoforms. Additional post-translational modifications and calcium activation can regulate the degree of titin-derived static tension¹⁰².

Summary

Problem:

Despite evidence of respiratory muscle weakness in patients with HCM, the responsible mechanism is still a matter of debate. Most of the literature supporting impaired respiratory function are based on rodent models with surgically induced congestive heart failure. Though CHF is one of the most debilitating symptoms of HCM, pathophysiology of HCM is so diverse that patients affected never report similar clinical manifestations. Thus, to understand the complete mechanism for respiratory weakness in HCM, it is important to study how the HCM mutations and progressing cardiac disease affects the diaphragm muscle function. Additionally, since the phenotypic expression of HCM mutation, the R403Q mutation, in particular, varies depending on the dominant cardiac myosin isoform in the species, selection of an appropriate animal model that closely resembles human cardiac myosin composition is important.

Rationale:

The following experimental study aims to evaluate the respiratory adaptations induced in HCM. This will be achieved by studying the contractile properties of the diaphragm muscle fibres in the rabbits with R403Q mutation induced HCM. To investigate whether alternations in the respiratory musculature associated with R403Q mutation are intrinsic to the muscle and not secondary to neural adaptive response to the increased oxygen drive, it is necessary to evaluate the contractile properties of the diaphragm muscle fibre independently. Thus, by isolating the study to isolated muscle fibre we can isolate the mechanism intrinsic to the diaphragm muscle itself.

Therefore, the goals of this study were twofold: (i) to examine if respiratory muscle weakness was present in rabbits with the R403Q mutation, and (ii) to examine the mechanism responsible for the alteration of force.

Our hypotheses are:

1. Diaphragm isolated from R403Q rabbits will be weaker than diaphragm isolated from wild-type rabbits.
2. The weakness observed in the R403Q myofibrils will be due to alterations in crossbridge kinetics of the muscle contractile unit.

CHAPTER II:
EXPERIMENTAL ARTICLE

ABSTRACT

Background: Hypertrophic cardiomyopathy (HCM), induced by a point mutation at residue 403 (R403Q), is one of the most lethal inherited cardiovascular diseases. Respiratory muscles weakness is frequently reported as secondary but independent mortality predictor in patients with cardiomyopathy, yet the mechanism of diaphragm weakness is not yet properly understood. In this study, we investigated the alterations in contractile properties of respiratory muscle diaphragm in hypertrophic cardiomyopathy, using a rabbit model with R403Q mutation. We hypothesised that genetically modified R403Q rabbits will show lower force recordings than the age-matched wild-type (WT) rabbits.

Method: Five sets of experiments were performed on isolated skinned diaphragm muscle fibres of WT and R403Q rabbits, to assess force development, redevelopment, enhancement (crossbridge kinetics) and passive forces between the two experimental groups.

Results: We found that the R403Q fibres were 11.21% weaker for specific force and 33.10% weaker when normalised to the crosssectional area of the fibres, compared with WT ($P < 0.05$). These fibres presented with similar kinetics for force redevelopment (k_{tr}) and unloaded shortening velocities (V_{max}). Also, R403Q fibres also reported 28.38% and 34.48% drop in force during stretch and force enhancement following stretch ($P < 0.05$). However, there was no difference in the passive force – SL relation between the two groups. In accordance with our hypothesis the diaphragm fibres from R403Q rabbits produce lower absolute and specific forces compared to WT.

Conclusion: In accordance with our hypothesis the diaphragm fibres from R403Q rabbits produce lower force and are weaker than WT and these alterations could be the result of altered crossbridge kinetics and calcium sensitivity.

INTRODUCTION

Hypertrophic cardiomyopathy (HCM), inherited as an autosomal dominant trait²⁸ is characterised by hypertrophy of the heart and is accompanied by asymmetric thickening of cardiac walls, a decrease in cardiac chamber size and impaired muscle relaxation^{14,31,33}. Histologically, the HCM related mutations in cardiac sarcomeric protein particularly affect the cardiac ventricles and may lead to cardiac muscle fibrosis and cardiac disarray in later years¹¹⁰. In addition to cardiac symptoms, patients with cardiomyopathies usually report impaired exercise capacity and dyspnea, associated with significant altered respiratory musculature^{6,22,50,55}. Inspiratory muscle weakness and reduced maximal inspiratory pressure, secondary to chronic heart failure, has been identified as an independent predictor of mortality in patients with hypertrophic cardiomyopathy (HCM)^{9,50,58}.

The diaphragm is the most important respiratory muscle and like the heart, it contracts and relaxes continuously throughout life. Several functional and metabolic studies of diaphragm muscles in conditions of cardiomyopathy have reported a decrease in muscle strength, as well as a consistent fibre type redistribution, from fast glycolytic towards slow oxidative fibres^{6,25,49}. These studies report a decreased force generation during maximal isometric contraction^{10,111} and changes in intracellular calcium regulation^{17,112,113}, which may underlie the mechanisms for intrinsic contractile dysfunction of the diaphragm in cardiomyopathic conditions.

Clinically, the vast heterogeneity of symptoms in individuals with HCM ranges from no symptom to ventricular arrhythmias and heart failure^{33,114,115}. The mutation of arginine to glutamine at amino acid 403(R403Q) in the β -myosin heavy chain (MHC) that leads to cardiomyopathy has been extensively studied¹¹⁶. Most of the data on R403Q mutation is based on

research on rodent models¹¹⁷⁻¹²⁰. However, there is a predominance of α -MHC in the myocardium of the mice, which differs considerably from humans. Recent studies by Lowey et al using R403Q mice model showed a strong dependence of the MHC isoforms affected in the contractile function; the α MHC and the β MHC present considerable differences in the characteristics of the cardiomyopathy^{40,41,121}. Most specifically, the heart with the α MHC backbone presents a gain in function, while the heart with the β MHC presents a loss in function. Such difference may lead to different effects on the diaphragm muscles, as a higher or lower blood flow will lead to different adaptations of the respiratory pathway.

In this study, we used a rabbit model for R403Q, which is better suited for understanding the mechanisms of HCM in humans than the mice, as the sarcomeric myosin composition in rabbits is marked by predominant expression of β -MHC in ventricles, same as in humans¹²². The similarities in heart rates and cardiac size also make the rabbit model ideal for most physiological studies^{33,123,124}. We isolated diaphragm muscle fibres from R403Q rabbit models and performed experiments with single fibres to test the hypothesis that the diaphragm contractile functions are altered because of HCM.

METHODS

Muscle fibre preparation

Small bundles of rabbit diaphragm muscles (3-4 cm) were dissected, tied to wooden sticks and chemically permeabilized according to standard procedure^{84,88}. These muscles were then soaked in rigor solution (pH = 7.0) for 4 hours, after which the samples were transferred to a rigor: glycerol (50:50) solution overnight. The samples were then transferred to a new rigor: glycerol solution with an additional mixture of protease inhibitors (Roche Diagnostics, USA) and stored in

a freezer (-20°C) for at least seven days. The protocol was approved by the McGill University Animal Care Committee (protocol #5227) and complied with the guidelines of the Canadian Council on Animal Care.

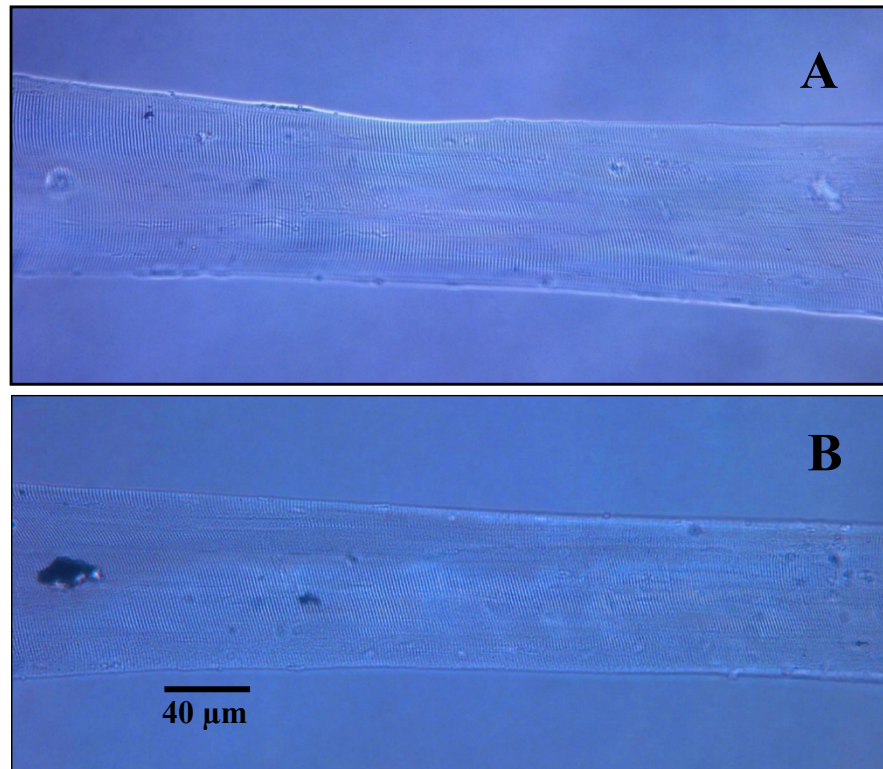


Figure 7: Photographs of single muscle fibres of the diaphragm in the experimental chamber. A typical diaphragm fibre isolated from a wild type (WT) rabbit (A) and from the diaphragm of a R403Q rabbit (B). There is no visible difference in the striation pattern and structure of the fibre between the two groups.

On the day of the experiment, sliced sections of the sample were transferred to fresh rigor solution in 1.5 mL eppendorf tube and placed in the fridge for an hour to defrost. The thawed sample was further dissected (~4 mm in length) and fine single muscle fibres were extracted in relaxing solution (pH = 7.0) (Figure 7). The fibres were fixed with T-shaped aluminium foil clips

and transferred to a temperature-controlled experimental chamber, hooked between a force transducer (403A, Aurora Scientific, Toronto, Canada) and a length controller (Model 312B, Aurora Scientific).

Solutions

The rigor solution (pH 7.0) was composed of (in mM): 50 Tris, 100 KCl, 2 MgCl₂ and 1 EGTA. The relaxin solution for dissection (pH 7.0) was composed of (in mM): 100 KCL, 2 EGTA, 20 Imidazole, 4 ATP and 7 MgCl₂. The activating solution was composed of (in mM): 20 imidazole, 14.5 creatine phosphate, 7 EGTA, 4 MgATP, 1 free Mg²⁺, 32 μM of free Ca²⁺ and KCL to adjust the ionic strength to 180 mM. A preactivating solution (pH 7.0, pCa²⁺ 9.0) composed of (in mM): 68 KCl, 0.5 EGTA, 20 Imidazole, 14.5 PCr, 4.83 ATP, 0.00137 CaCl₂, 5.41 MgCl₂ and 6.5 HDTA (pH 7.0, pCa²⁺ 9.0) was used immediately before activation of fibres. The final concentrations of each metal-ligand complex were calculated using a computer program¹²⁵

Experimental Protocol

In the experimental chamber, the average SL of the fibre in relaxing solution was calculated using a high-speed video system (HVSL, Aurora Scientific 901A, Toronto, Canada). Images from selected region of the fibre were used to calculate SL by Fast Fourier Transform (FFT) analysis, which is based on the striation spacing pattern of the dark and light bands of myosin and actin, respectively. The length and diameter of the fibre were measured using CCD camera (Go-3, QImaging, USA; pixel size: 3.2 μm×3.2 μm). All experiments were performed at 10°C.

Every muscle fibre underwent five experiments protocols during the trial study. The initial SL of the fibre was adjusted to 2.5μm (optimal length; L_o) before every experiment. For the first

test, the fibre was activated to produce maximal isometric force. The contraction was induced by transferring the single fibre preparation to the bath with a pre-activating solution for 5 s, then to activating solution (pCa^{2+} 4.5) for 10 s before allowing deactivation in relaxing solution (pCa^{2+}).

The second experiment measured the rate of isometric force re-development (k_{tr}). The fibre was activated isometrically at pCa^{2+} 4.5, and after full force development, the fibre was shortened by 15% L_o with $10 L_o \cdot s^{-1}$ ramp, reducing the force to zero. This momentarily reduces the dynamic stiffness and suddenly dissociates all attached crossbridges. The shortening is followed by a rapid re-stretch ($500 L_o \cdot s^{-1}$) to initial L_o , forcing disengagement of any remaining attached crossbridges. Force re-development after the shortening-stretch protocol is directly related to the re-attachment of myosin to actin.

The third experiment was performed to measure force enhancement during and after stretch. The fibre was first activated at pCa^{2+} 4.5 and when the force was fully developed, a ramp stretch of 10% L_o was applied at $5 L_o \cdot SL^{-1} \cdot s^{-1}$. The fibre was restored to its original length after 10 seconds and then allowed to relax in the relaxin solution. Residual force enhancement was calculated as the difference between force measured after an active stretch and force produced during isometric contraction¹⁰¹.

The fourth experiment measured unloaded shortening velocity (V_{max}) using slack test method. The fibre underwent four separate slack tests, corresponding to length steps of 5, 10, 15 and 20% L_o . The activated fibre was subjected to predetermine slack step rapidly imposed at 2 ms, allowing the muscle to slacken and the force dropped to zero. The force redeveloped over time in proportion to the shortening length imposed. Following 10 s the fibre was re-stretch to its initial L_o , and then transferred to relaxin for deactivation; the SL was readjusted prior to subsequent

activation. The time required for re-development of force, which was relative to the step length applied, was plotted and the slope of the linear regression fitting the data represented the V_{\max} (in $L_0 \cdot s^{-1}$).

For the last protocol, fibres underwent 10 consecutive step-stretches in relaxing solution (amplitude of stretch: 10 % initial L_0 , duration 1 s, pauses between stretches: 3 seconds, 10 steps) the protocol was developed for comparison of passive forces-SL relation ¹⁰¹.

The force and length traces were recorded throughout all the experiments at a rate of 10000 Hz. The maximal force generated by a fibre was measured at the end of the activation period after steady-state stabilisation was achieved. In all trials, control contractions at SL of 2.5 μm were elicited at the end of the experiments, and if isometric forces decreased by >15% in relation to the first isometric contraction, or when the striation pattern corresponding to the SL became unclear, the experiments were ended and the data was not used.

Data analysis

Force re-development (k_{tr}) was analysed using the following bi-exponential equation:

$$\mathbf{F} = \{ \mathbf{a} * [\mathbf{1} - e^{(-k_{tr} * t)} - e^{(-l * t)}] + \mathbf{b} \}$$

where 'F' is force, 'a' is the amplitude of the exponentials, 't' is time, ' k_{tr} ' the first exponential constant, ' l ' the second exponential constant, and 'b' is the initial force value.

The forces during and after stretch were also calculated as the difference in the peak force recorded during and after stretch and the isometric force produced by the fibre.

The passive force-SL relation of the two groups was estimated by comparing the peak forces during step stretches and the passive forces recorded after the stretches.

Statistics

The comparisons between the two groups were made using T-test. When appropriate, post hoc analyses were made using Man Whitney's U-test was performed after independent t-test.

The passive force-SL relationship was analysed using a two-way ANOVA, where the first factor was the type of fibre used (WT or R403Q) and the second factor was the amount of stretch that the fibres endured during the protocol. Post hoc analysis using Holm-Sidak method was performed. A significance level of $p < 0.05$ was used for all comparisons. All values are presented as mean \pm S.E.M.

RESULTS

Isometric force: Figure 8 shows typical force readings recorded during isometric contraction of single muscle fibre isolated from the diaphragm muscles of WT and R403Q rabbits, respectively. The specific force obtained after normalisation with the cross-sectional area (CSA) was 33.10% lower in R403Q fibres ($p = 0.045$) when compared with WT. Data for CSA of permeabilized diaphragm muscle fibres, measured assuming circular symmetry, is presented in Table 1. The CSA were different across both the groups.

	WT	R403Q
Force (mN)	0.758 \pm 0.155	0.673 \pm 0.0902
CSA (mm²)	6.09*10 ⁻³ \pm 0.72*10 ⁻³	8.33*10 ⁻³ \pm 0.92*10 ⁻³
Specific Force (mN/mm²)	117.85 \pm 13.41	78.82 \pm 12.67*

* Significantly different from WT (Mean \pm SE)

Table 1: Fibre segment cross-sectional area (CSA), force and specific force.

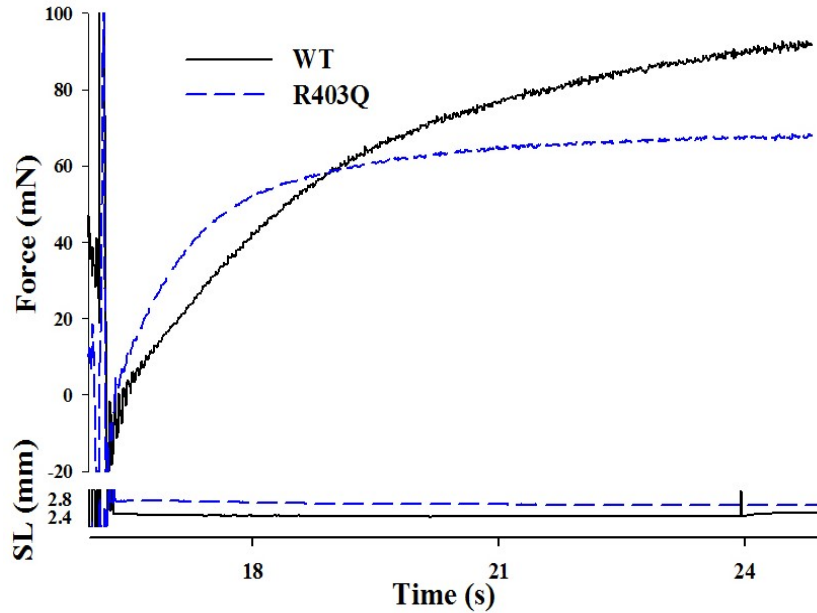


Figure 8: Isometric contractions recorded during typical experiment with WT and R403Q diaphragm fibres. These traces are normalized to crosssectional area of the respective fibre. Note that the isometric force recorded for R403Q is lower than the WT.

Rate of force redevelopment (k_{tr}): Figure 9(A) shows typical force tracings recorded from single diaphragm muscles isolated from WT and R403Q, respectively. Although the isometric forces are considerably lower for R403Q, the slope of force redevelopment is similar for both WT and R403Q (indicated by the arrows). The similar k_{tr} suggests that there is no difference in the crossbridge turnover after the shortening-stretch protocol.

When the results are plotted together (figure 9(B)), statistical analysis confirmed these findings; the k_{tr} did not differ between the two groups, with a k_{tr} of $0.87/\text{sec} \pm 0.35$ for the WT fibres and $1.57/\text{sec} \pm 0.59$ for the R403Q fibres ($P > 0.05$).

Force enhancement during and after stretch of activated fibres: The force produced at the peak of the stretch (critical force, P_c), and the force enhancement after stretch, were higher than

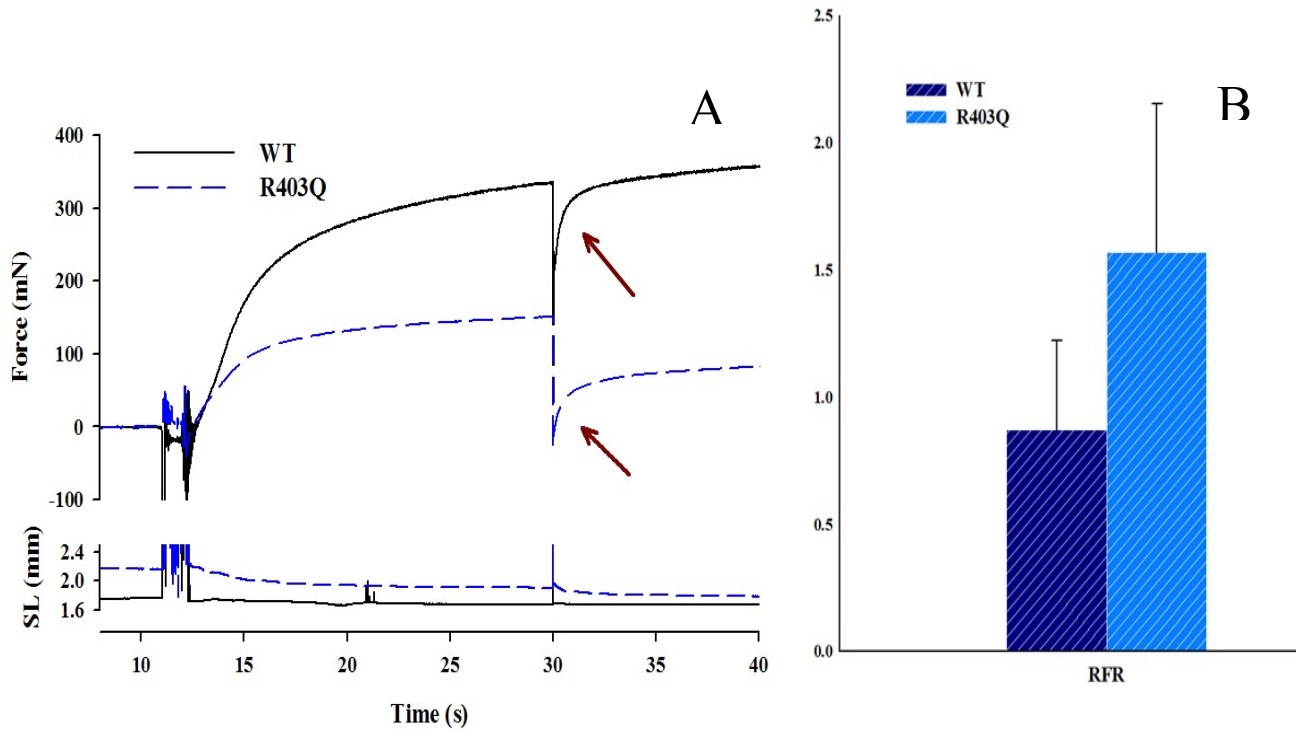


Figure 9: (A) Rate of force redevelopment (k_{tr}). Typical force traces in experiments measuring k_{tr} in WT and R403Q muscle fibres. (B) Mean values k_{tr} recorded for both groups. Solid bars are the mean data recorded while the extended bars represent the standard error. Note that higher k_{tr} would suggest that R403Q redevelops force faster than the wild type, but there is no statistical difference in the k_{tr} (Mean \pm SE) of both the groups.

the steady state force produced during isometric contraction, for both fibres. Figure 10 shows typical force traces recorded, note that the steady-state force obtained after stretch is higher than isometric force produced by WT and R403Q fibres. Force enhancement after stretch, calculated as the difference between this steady stated force and force produced during pure isometric contraction was lower for R403Q when compared to WT. Statistically, the force enhancement after stretch was 34.49% lower in R403Q ($39.92 \text{ mN/mm}^2 \pm 4.80$) when compared to WT ($60.92 \text{ mN/mm}^2 \pm 6.08$), and the P_c was 28.37% lower ($P < 0.05$), in R403Q ($474.93 \text{ mN/mm}^2 \pm 63.19$) than WT ($663.07 \text{ mN/mm}^2 \pm 51.15$) as shown in figure 11(A).

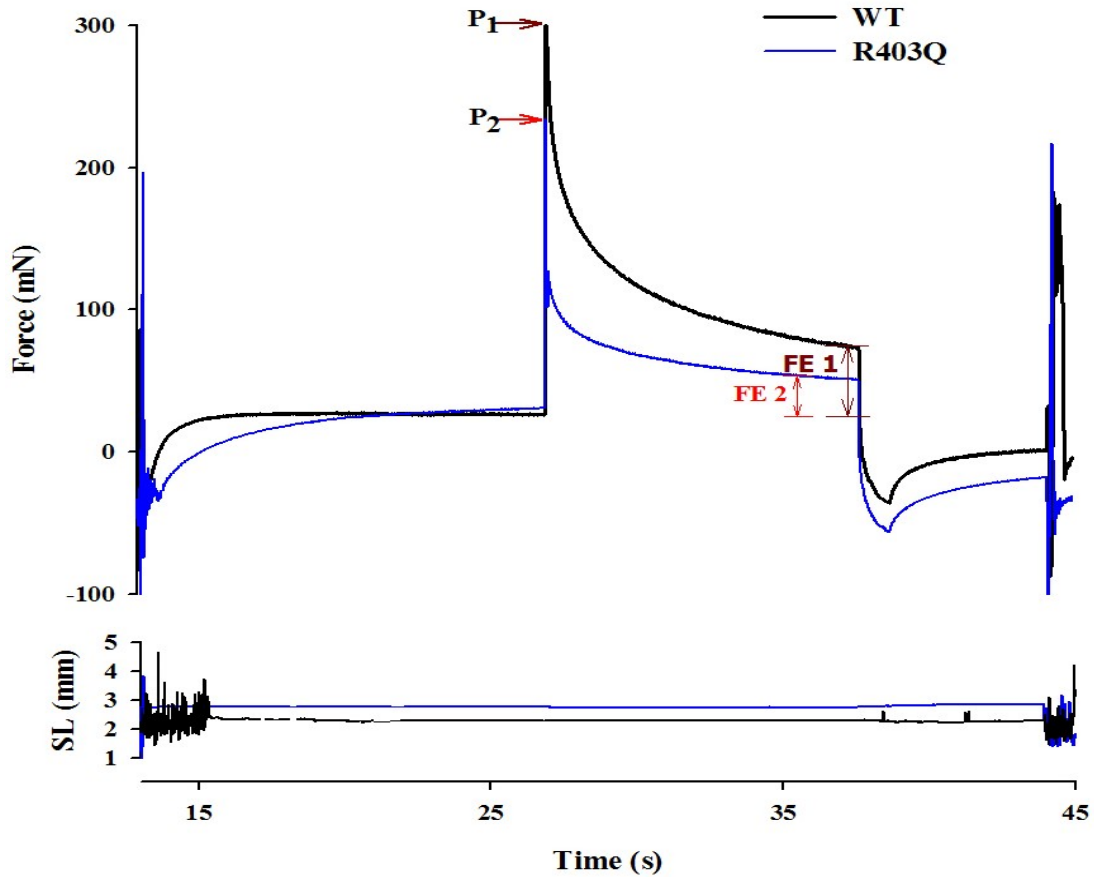


Figure 10: Typical force traces of single muscle fibres isolated from WT (1) and R403Q (2) rabbits, showing force enhancement during stretch (P_1 and P_2) and after stretch (FE 1 and FE 2). The isometric force and the peak force during the active stretch are lower in the R403Q fibre (P_2) when compared to the WT fibre (P_1). Force enhancement after stretch, calculated as the difference in force recorded after stretch and the isometric force produced during contraction, was lower for the rabbits with R403Q mutation (FE 2) relative to WT (FE 1)

Unloaded shortening velocity (V_{max}): Figure 12. shows typical data recorded for slack tests performed on diaphragm fibres isolated from R403Q and WT rabbits. There was no statistical difference in the unloaded shortening velocity measured with the slack test method between the two groups, with a V_{max} of $0.42 \text{ Lo/s} \pm 0.12$ for WT and $0.40 \text{ Lo/s} \pm 0.08$ for R403Q ($P > 0.05$)

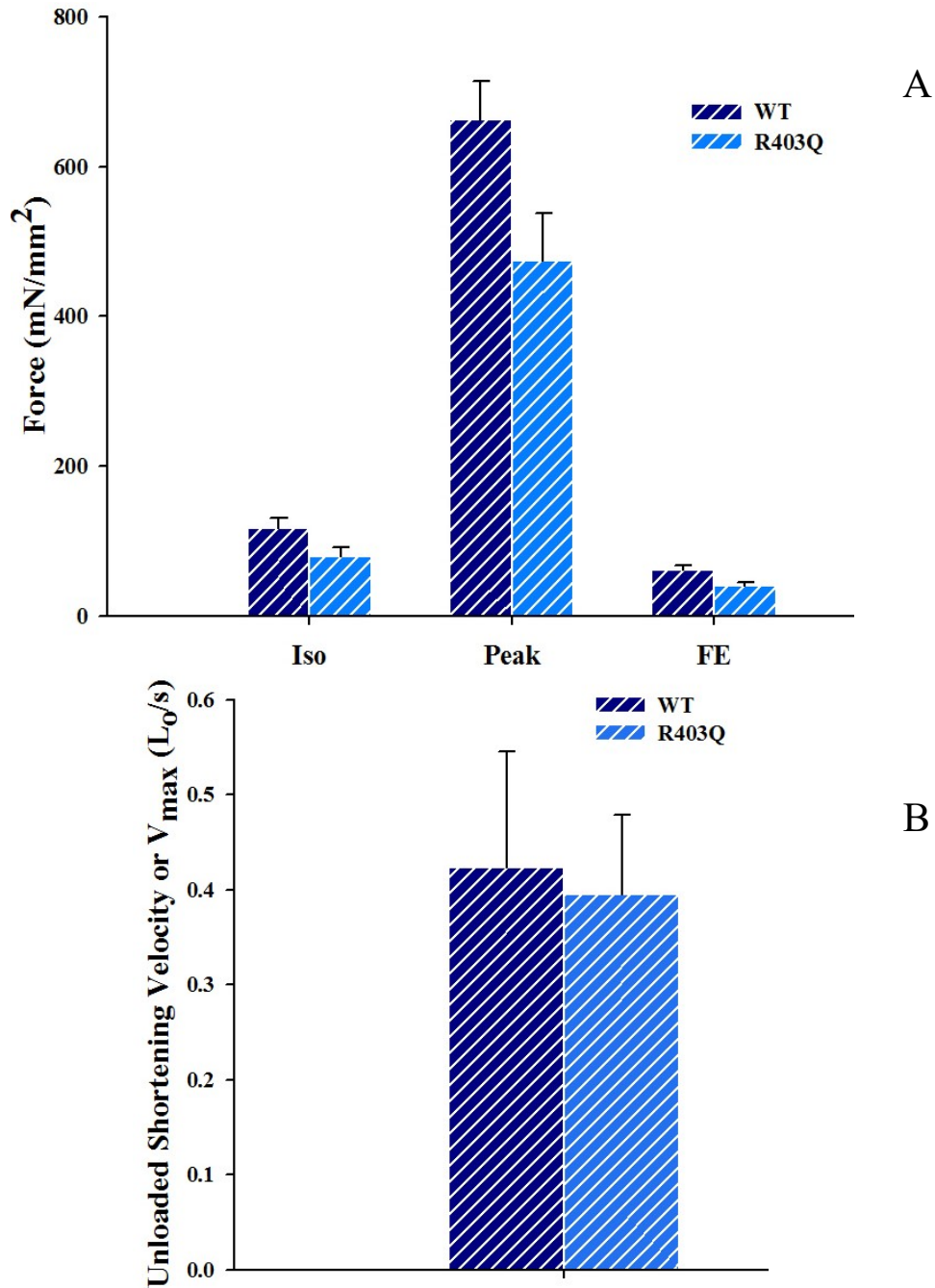


Figure 11: (A) Mean values for force recorded during isometric contraction (Iso), point of maximal stretch (Peak) and force enhancement observed after stretch (FE). The force enhancement measured during and after stretch of activated fibre is significantly lower in diaphragm fibres extracted from R403Q when compared to WT ($P < 0.05$). (B) Mean unloaded shortening velocity. There is no statistical difference between unloaded shortening velocity (V_{\max}) computed for the two groups (Mean \pm SE).

as evident in figure 11(B).

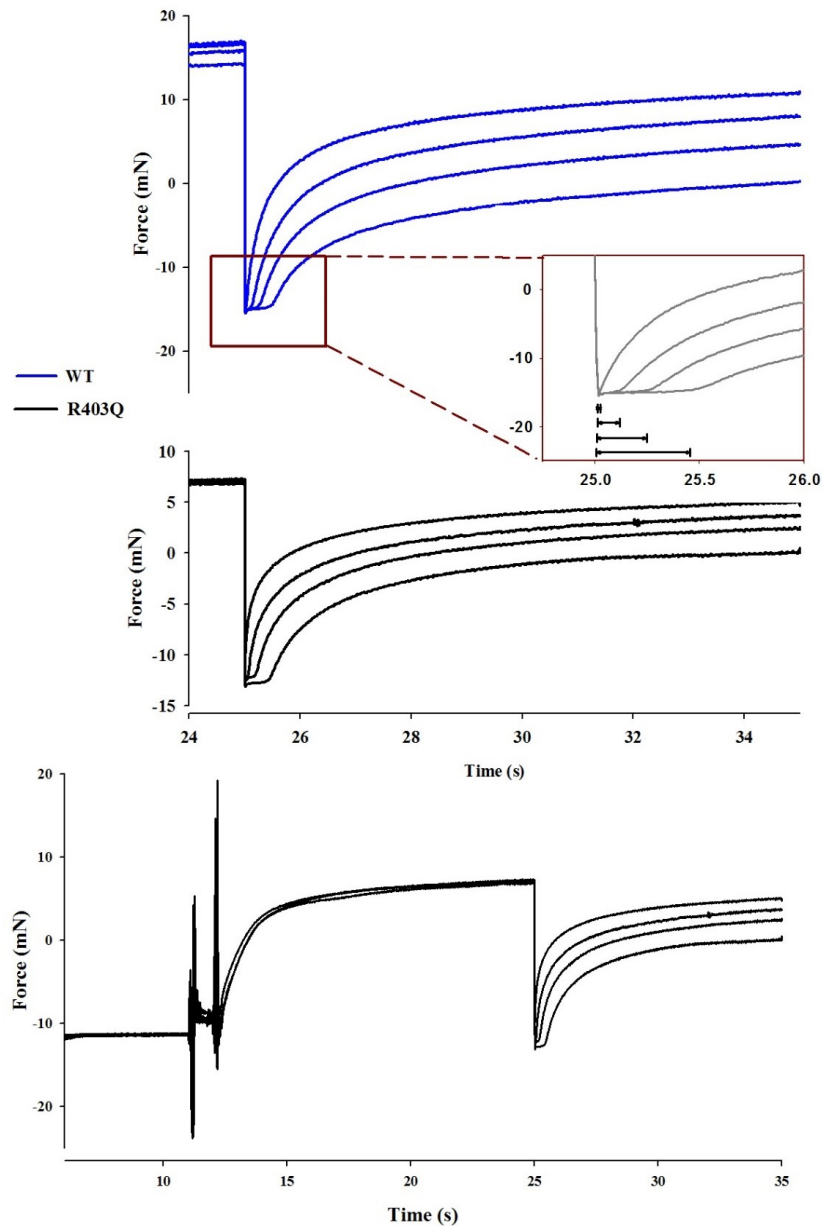


Figure 12: Raw data traces showing experiments performed for evaluation of V_{\max} in diaphragm muscle fibre extracted from WT and R403Q fibres. Four separate slack tests, corresponding to length steps of 5, 10, 15, 25% L_0 , were performed on each fibre. The time required for the force to redevelop was plotted relative to the imposed length step. V_{\max} was derived as the slope of the first order least squares regression line fitting the data. Inset: Zoomed view of the unloaded shortening velocity traces.

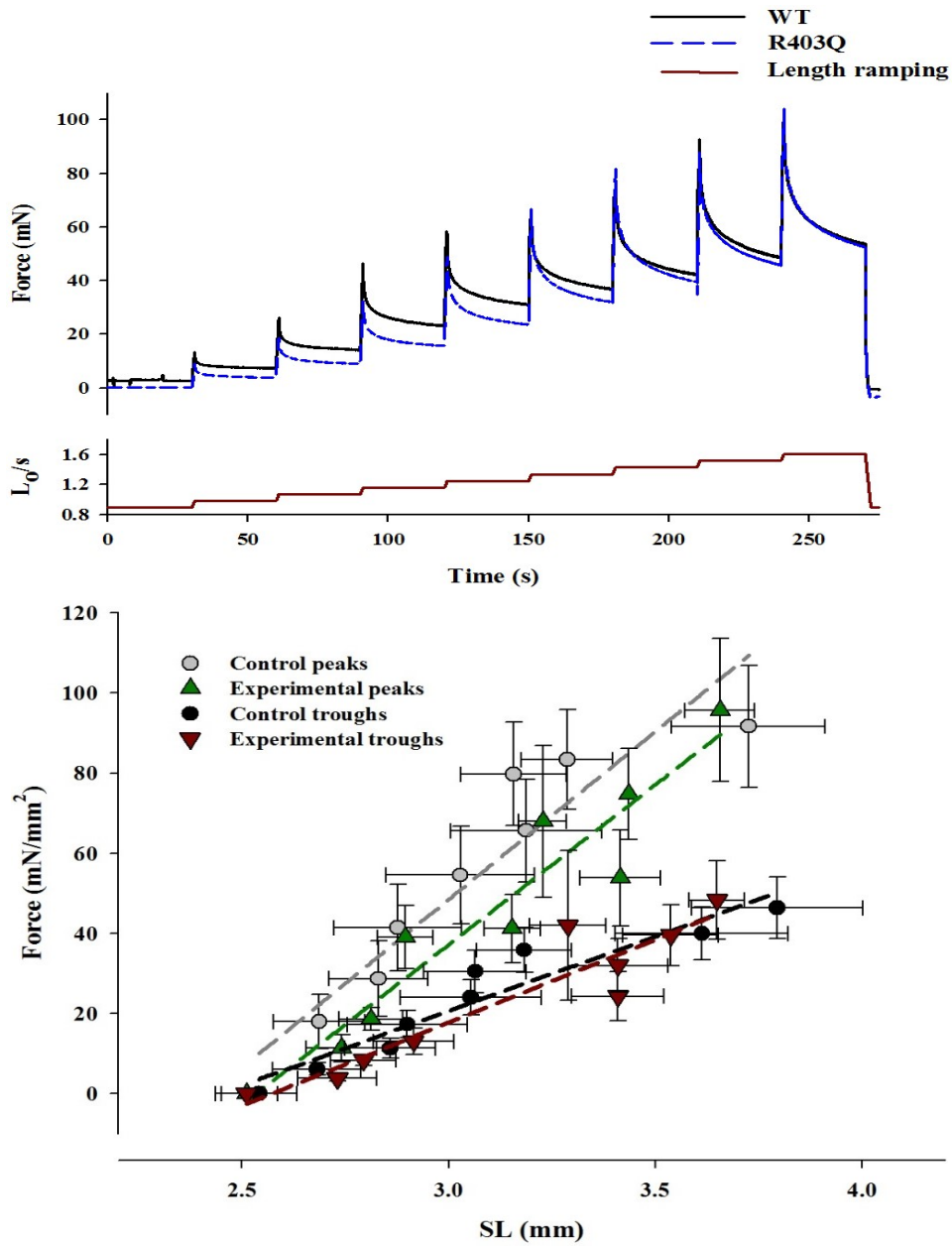


Figure 13:(A) Raw data traces for passive force – SL relation of WT and R403Q diaphragm muscle fibres. Consecutive stretches performed at pCa^{2+} 9.0 with individual fibres isolated from the diaphragm of WT and R403Q rabbits. The forces produced during and after stretches are the same for both the group. The bottom panel shows the step length ramp imposed on the fibres for this protocol. (B) Means (\pm SE) of Passive force - SL relation for all fibres investigated in this study. Both the peak forces during stretches (triangles – peaks) and the passive forces after stretches (circles – trough) were calculated to be similar between the groups.

Passive force - SL relation: Figure 13(A) shows a passive force – SL relation for both WT and R403Q fibres investigated in this study. Note that critical force recorded during consecutive stretches were similar for both R403Q and WT.

Holm-Sidak posthoc analysis following two-way ANOVA revealed that there was no significant difference in the passive force traces of WT and R403Q fibres. Interestingly, the steady-state forces attained during stretches were lower in fibres isolated from R403Q diaphragm muscle. However, despite subjecting the fibres to high magnitude of stretches, the absence group and stretch length interaction established that there was no statistical difference in the passive force-SL relation between the two groups ($P>0.05$; figure 13(B)).

DISCUSSION

This study is the first to investigate the contractile properties of diaphragm muscle fibres isolated from the R403Q rabbit, a cardiomyopathy model that resembles the human disease. We investigated the extent to which this cardiac mutation alters the force, velocity of contraction and crossbridge kinetics of the diaphragm. The data from our study shows that the diaphragm fibres of R403Q rabbits are weaker in comparison to WT myofibrils. In addition to a reduced force generation, these fibres produced a lower force in response to stretch. Taken together with similar values for rate of force redevelopment, maximal shortening velocity, and passive forces, these findings indicate that the muscle weakness in R403Q rabbit model is not associated with impairment in crossbridge kinetics.

Comparisons with other studies:

Our findings are similar to studies on CHF^{6,22,26,59} that reported a loss in maximal force generation of the diaphragm secondary to heart failure in rodents. In one of these studies, Van Hees et. al.²⁶ observed lower values for rates of force redevelopment (k_{tr}) in diaphragm isolated from rats with surgically induced CHF, in addition to the reduced maximal specific force. This change was accompanied by a decrease in α -MHC content as well. Though we observed a decrease in maximal force production in our study, there was no difference in k_{tr} of R403Q diaphragm relative to wild-type rabbit, even though the mutation and animal selected was a better model of HCM for cardiomyopathy.

In a previous study from our laboratory, Ribeiro et.al²⁴ reported an increase in the maximal force production and faster rate of relaxation in the diaphragm of affected animals. A knockout mouse model with cardiac-specific deletion of arginyl-tRNA-protein transferase was employed to reproduce symptoms of cardiomyopathy and CHF. However, even in this study, there was no difference in k_{tr} and passive forces in the fibres isolated from diaphragm muscles, despite increased loading conditions secondary to chronic cardiac failure.

Causes of impaired diaphragm muscle fibre contractility:

The specific force of fibres isolated from R403Q was lower than that of wild-type. Similar values for rate of force redevelopment and maximum velocity of shortening ruled out the differences in the in the rate of crossbridge turnover and the speed of myosin crossbridges cycling at zero load. Comparable values for passive force-SL relation (at pCa^{2+} 9.00), between the two groups, may rule out the involvement of titin in diaphragm weakness. However, it may be that a Ca^{2+} dependent increase in the stiffness of titin^{104,126} may be responsible for changes observed in

the total force produced by the diaphragm fibres. Cornachione and Rassier¹⁰¹ reported an upward shift in the passive force-SL relation in the presence of Ca^{2+} , even after blocking the crossbridge interactions by removal of the thin filament, and it would be important to study the passive forces-SL relation in the presence of Ca^{2+} .

Interestingly, the muscle fibres from R403Q diaphragm produced lower force in response to stretch after activation both during and after stretch relative to fibres from wild-type. The critical force (\mathbf{P}_c) was 34% lower for R403Q relative to WT. The \mathbf{P}_c is associated with the force at which the attached crossbridges reach their maximum extension, before detaching from actin or the ‘pre-power stroke’ phase⁸⁰. This suggests that the pre-power stroke crossbridges are unable to sustain the strain of stretching^{81,82}, thereby resulting in lower \mathbf{P}_c observed in the fibre. Since the \mathbf{P}_c was low to begin with, the force enhancement observed after stretch was also reduced relative to wild type.

Research on patients with early onset cardiomyopathy has indicated that some autosomal dominant missense mutation also affects the skeletal muscles^{127,128}. Fananapazir et. al. have demonstrated that the patients with the R403Q mutation in the β -MHC also show alterations in the myofibrillar structure, even in skeletal muscles¹²⁸. They reported variations in the fibre sizes and histochemical alterations in psoas muscle biopsies of patients with HCM. These studies suggest that mutations resulting in cardiomyopathy also affect the sarcomeric integrity of skeletal muscles. Such alterations may affect force enhancement during and after stretch⁷², and this could provide an explanation for the inability of diaphragm muscle fibre to resist to the strain imposed by a stretch.

Taken together, these data suggest that intrinsic contractile dysfunction of the diaphragm, contributes to inspiratory muscle weakness in HCM. This inspiratory muscle weakness may be

secondary to alterations in the stabilising proteins, due to which the muscle is unable to develop tension thereby resulting in lower force production by the contractile apparatus.

Limitations

In the present study, we compared the contractile properties of diaphragm muscle in cardiomyopathic rabbits with the R403Q mutation. Although this animal model has better genetic and clinical similarities with human than mice models, we lack information on the neurohormonal profile of the rabbits following cardiomyopathy.

Conclusion

This results of this study show a lower force production in diaphragm single fibres of rabbits with an R403Q mutation in the heart. The results also suggest that HCM indirectly affects contractile proteins and passive structures of the diaphragm muscle. However, these abnormalities were not accompanied by changes in k_{tr} and V_{max} , suggesting that the mutation may not affect crossbridge kinetics. Instead, the weakness could be arising from the decrease in passive forces originating from titin related stiffness in the diseased muscle fibre and non-crossbridges structures.

CHAPTER III:
CONCLUSION AND FUTURE DIRECTIONS

The results of this thesis show that diaphragm muscle fibres in rabbits, with familial hypertrophic cardiomyopathy resulting from R403Q mutation, are weaker in comparison to wild-type rabbits. Lower forces in response to stretch suggest that the weakness may be attributed to the passive structures within the muscle. Though R403Q mutation is the most extensively researched mutation of HCM, this is the first study to investigate the contractile changes in the respiratory muscle of the specific mutation in a large mammal. This study is a step closer to understanding HCM further studies will be required to elucidate the exact mechanism.

There are two main directions to be developed from this thesis for future studies. First, although this thesis was successful in establishing respiratory weakness in HCM, further muscle biophysics research will be needed to elucidate the exact mechanism responsible for the observed drop in forces. Future research testing for calcium sensitivity in R403Q would help us understand the muscle fibre's response while activation, contraction as well as relaxation. The drop in isometric force and the force enhancement observed in this study would be justified if the R403Q fibres have developed a tolerance to Ca^{2+} and hence need more calcium ions to illicit isometric contractile force.

Additionally, MHC isoform comparisons and titin isoform comparison of cardiac muscles of R403Q rabbits have established fibre-type shifting and lower cardiac functionality. Changes in the MHC proteins could explain the drop in isometric force. Investigating the physiological alterations in the diaphragm muscle such as fibre typing and mitochondrial function analysis, among other, can give a complete view of the underlying adaptations to HCM.

One of the main clinical implication of this study is that respiratory weakness reported in patients with HCM is independent of the underlying cardiac condition. Since HCM screening is

encouraged right from a very young age, respiratory muscle training can improve the survival rate of the patient after diagnosis.

REFERENCES:

- 1 Ottenheijm, C. A., van Hees, H. W., Heunks, L. M. & Granzier, H. Titin-based mechanosensing and signaling: role in diaphragm atrophy during unloading? *American journal of physiology. Lung cellular and molecular physiology* **300**, L161-166, doi:10.1152/ajplung.00288.2010 (2011).
- 2 Edman, K. The velocity of unloaded shortening and its relation to sarcomere length and isometric force in vertebrate muscle fibres. *The Journal of physiology* **291**, 143 (1979).
- 3 Edman, K. Double-hyperbolic force-velocity relation in frog muscle fibres. *The Journal of physiology* **404**, 301 (1988).
- 4 Poggesi, C., Tesi, C. & Stehle, R. Sarcomeric determinants of striated muscle relaxation kinetics. *Pflugers Archiv : European journal of physiology* **449**, 505-517, doi:10.1007/s00424-004-1363-5 (2005).
- 5 Minozzo, F. C. & Lira, C. A. Muscle residual force enhancement: a brief review. *Clinics (Sao Paulo, Brazil)* **68**, 269-274 (2013).
- 6 Howell, S. *et al.* Congestive heart failure: differential adaptation of the diaphragm and latissimus dorsi. *Journal of Applied Physiology* **79**, 389-397 (1995).
- 7 Mancini, D. M., Henson, D., LaManca, J. & Levine, S. Respiratory muscle function and dyspnea in patients with chronic congestive heart failure. *Circulation* **86**, 909-918 (1992).
- 8 De Sousa, E. *et al.* Dual influence of disease and increased load on diaphragm muscle in heart failure. *Journal of Molecular and Cellular Cardiology* **33**, 699-710, doi:10.1006/jmcc.2000.1336 (2001).
- 9 Hughes, P. D. *et al.* Diaphragm Strength In Chronic Heart Failure. *American Journal of Respiratory and Critical Care Medicine* **160**, 529-534, doi:10.1164/ajrccm.160.2.9810081 (1999).
- 10 Lecarpentier, Y. *et al.* Mechanics, energetics, and crossbridge kinetics of rabbit diaphragm during congestive heart failure. *FASEB journal : official publication of the Federation of American Societies for Experimental Biology* **12**, 981-989 (1998).

- 11 Kemp, G. J. *et al.* Abnormalities in exercising skeletal muscle in congestive heart failure can be explained in terms of decreased mitochondrial ATP synthesis, reduced metabolic efficiency, and increased glycogenolysis. *Heart* **76**, 35-41 (1996).
- 12 Belus, A. *et al.* The familial hypertrophic cardiomyopathy-associated myosin mutation R403Q accelerates tension generation and relaxation of human cardiac myofibrils. *The Journal of physiology* **586**, 3639-3644, doi:10.1113/jphysiol.2008.155952 (2008).
- 13 Bernstein, D. Exercise assessment of transgenic models of human cardiovascular disease. *Physiological genomics* **13**, 217-226, doi:10.1152/physiolgenomics.00188.2002 (2003).
- 14 Chuan, P., Sivaramakrishnan, S., Ashley E , A. & Spudich J , A. Cell-Intrinsic Functional Effects of the α -Cardiac Myosin Arg-403-Gln Mutation in Familial Hypertrophic Cardiomyopathy. *Biophysical Journal* **102**, 2782-2790, doi:10.1016/j.bpj.2012.04.049 (2012).
- 15 Daganou, M., Dimopoulou, I., Alivizatos, P. & Tzelepis, G. Pulmonary function and respiratory muscle strength in chronic heart failure: comparison between ischaemic and idiopathic dilated cardiomyopathy. *Heart* **81**, 618-620 (1999).
- 16 Debold, E. P. *et al.* Hypertrophic and dilated cardiomyopathy mutations differentially affect the molecular force generation of mouse alpha-cardiac myosin in the laser trap assay. *American journal of physiology. Heart and circulatory physiology* **293**, H284-291, doi:10.1152/ajpheart.00128.2007 (2007).
- 17 Dominguez, J. F. & Howell, S. Compartmental analysis of steady-state diaphragm Ca²⁺ kinetics in chronic congestive heart failure. *Cell Calcium* **33**, 163-174, doi:10.1016/S0143-4160(02)00208-7 (2003).
- 18 Eddinger, T., Moss, R. & Cassens, R. Fiber number and type composition in extensor digitorum longus, soleus, and diaphragm muscles with aging in Fisher 344 rats. *Journal of Histochemistry & Cytochemistry* **33**, 1033-1041 (1985).
- 19 Eddinger, T. J. & Moss, R. L. Mechanical properties of skinned single fibers of identified types from rat diaphragm. *Am J Physiol Cell Physiol* **253**, C210-C218 (1987).

- 20 Geiger, P. C., Cody, M. J., Macken, R. L. & Sieck, G. C. Maximum specific force depends on myosin heavy chain content in rat diaphragm muscle fibers. *Journal of Applied Physiology* **89**, 695-703 (2000).
- 21 Howell, S. *et al.* Congestive heart failure: differential adaptation of the diaphragm and latissimus dorsi. *Journal of applied physiology (Bethesda, Md. : 1985)* **79**, 389-397 (1995).
- 22 Lecarpentier, Y. *et al.* Impaired load dependence of diaphragm relaxation during congestive heart failure in the rabbit. *Journal of Applied Physiology* **87**, 1339-1345 (1999).
- 23 Hasenfuss, G. Animal models of human cardiovascular disease, heart failure and hypertrophy. *Cardiovascular research* **39**, 60-76 (1998).
- 24 Ribeiro, P. A. B. *et al.* Contractility of myofibrils from the heart and diaphragm muscles measured with atomic force cantilevers: Effects of heart-specific deletion of arginyl-tRNA-protein transferase. *International Journal of Cardiology* **168**, 3564-3571, doi:<http://dx.doi.org/10.1016/j.ijcard.2013.05.069> (2013).
- 25 Tikunov, B., Levine, S. & Mancini, D. Chronic congestive heart failure elicits adaptations of endurance exercise in diaphragmatic muscle. *Circulation* **95**, 910-916 (1997).
- 26 van Hees, H. W. H. *et al.* Diaphragm single-fiber weakness and loss of myosin in congestive heart failure rats. *American Journal of Physiology - Heart and Circulatory Physiology* **293**, H819-H828, doi:10.1152/ajpheart.00085.2007 (2007).
- 27 Elliott, P. *et al.* Classification of the cardiomyopathies: a position statement from the european society of cardiology working group on myocardial and pericardial diseases. *European Heart Journal*, doi:10.1093/eurheartj/ehm342 (2007).
- 28 Maron, B. J. Hypertrophic cardiomyopathy: a systematic review. *Jama* **287**, 1308-1320 (2002).
- 29 Braunwald, E. in *Hypertrophic Cardiomyopathy* Ch. 1, 1-8 (Springer, 2015).
- 30 Elliott, P. M. *et al.* 2014 ESC Guidelines on diagnosis and management of hypertrophic cardiomyopathy. *The Task Force for the Diagnosis and Management of Hypertrophic*

- Cardiomyopathy of the European Society of Cardiology (ESC)*, doi:10.1093/eurheartj/ehu284 (2014).
- 31 Harvey, P. A. & Leinwand, L. A. Cellular mechanisms of cardiomyopathy. *The Journal of cell biology* **194**, 355-365 (2011).
- 32 Fatkin, D. & Graham, R. M. Molecular Mechanisms of Inherited Cardiomyopathies. *Physiological Reviews* **82**, 945-980, doi:10.1152/physrev.00012.2002 (2002).
- 33 Shephard, R. & Semsarian, C. Role of animal models in HCM research. *Journal of cardiovascular translational research* **2**, 471-482 (2009).
- 34 Geisterfer-Lowrance, A. A. T. *et al.* A molecular basis for familial hypertrophic cardiomyopathy: A β cardiac myosin heavy chain gene missense mutation. *Cell* **62**, 999-1006, doi:[http://dx.doi.org/10.1016/0092-8674\(90\)90274-I](http://dx.doi.org/10.1016/0092-8674(90)90274-I) (1990).
- 35 Seidman, C. E. & Seidman, J. G. Gene mutations that cause familial hypertrophic cardiomyopathy. *Molecular cardiovascular medicine. New York: Scientific American*, 193-209 (1995).
- 36 Geisterfer-Lowrance, A. A. T. *et al.* A Mouse Model of Familial Hypertrophic Cardiomyopathy. *Science* **272**, 731-734, doi:10.1126/science.272.5262.731 (1996).
- 37 McConnell, B. K. *et al.* Comparison of two murine models of familial hypertrophic cardiomyopathy. *Circulation research* **88**, 383-389 (2001).
- 38 Georgakopoulos, D. *et al.* The pathogenesis of familial hypertrophic cardiomyopathy: early and evolving effects from an alpha-cardiac myosin heavy chain missense mutation. *Nature medicine* **5**, 327-330, doi:10.1038/6549 (1999).
- 39 Swynghedauw, B. Developmental and functional adaptation of contractile proteins in cardiac and skeletal muscles. *Physiol Rev* **66**, 710-771 (1986).
- 40 Lowey, S. *et al.* Functional effects of the hypertrophic cardiomyopathy R403Q mutation are different in an alpha- or beta-myosin heavy chain backbone. *The Journal of biological chemistry* **283**, 20579-20589, doi:10.1074/jbc.M800554200 (2008).

- 41 Lowey, S., Bretton, V., Gulick, J., Robbins, J. & Trybus, K. M. Transgenic mouse α - and β -cardiac myosins containing the R403Q mutation show isoform-dependent transient kinetic differences. *Journal of Biological Chemistry* **288**, 14780-14787 (2013).
- 42 Marian, A. J. *et al.* A transgenic rabbit model for human hypertrophic cardiomyopathy. *The Journal of clinical investigation* **104**, 1683-1692, doi:10.1172/jci7956 (1999).
- 43 Krishnan, B. & Wang, Y. Inspiratory Muscle Weakness and Dyspnea in Chronic Heart Failure¹⁻³. *Am Rev Respir Dis* **146**, 467-472 (1992).
- 44 Gehlbach, B. K. & Geppert, E. The Pulmonary Manifestations of Left Heart Failure. *Chest* **125**, 669-682, doi:<http://dx.doi.org/10.1378/chest.125.2.669> (2004).
- 45 Mancini, D. M., Ferraro, N., Nazzaro, D., Chance, B. & Wilson, J. R. Respiratory muscle deoxygenation during exercise in patients with heart failure demonstrated with near-infrared spectroscopy. *Journal of the American College of Cardiology* **18**, 492-498 (1991).
- 46 Hughes, P. D. *et al.* Diaphragm strength in chronic heart failure. *Am J Respir Crit Care Med* **160**, 529-534, doi:10.1164/ajrccm.160.2.9810081 (1999).
- 47 Zhu, E., Petrof, B. J., Gea, J., Comtois, N. & Grassino, A. E. Diaphragm muscle fiber injury after inspiratory resistive breathing. *American Journal of Respiratory and Critical Care Medicine* **155**, 1110-1116, doi:10.1164/ajrccm.155.3.9116995 (1997).
- 48 Lieber, R. L., Schmitz, M. C., Mishra, D. K. & Friden, J. Contractile and cellular remodeling in rabbit skeletal muscle after cyclic eccentric contractions. *Journal of applied physiology (Bethesda, Md. : 1985)* **77**, 1926-1934 (1994).
- 49 Tikunov, B. A., Mancini, D. & Levine, S. Changes in myofibrillar protein composition of human diaphragm elicited by congestive heart failure. *J Mol Cell Cardiol* **28**, 2537-2541, doi:10.1006/jmcc.1996.0245 (1996).
- 50 Meyer, F. J. *et al.* Respiratory muscle dysfunction in congestive heart failure: clinical correlation and prognostic significance. *Circulation* **103**, 2153-2158 (2001).

- 51 Müller-Höcker, J. *et al.* Fatal infantile mitochondrial cardiomyopathy and myopathy with heterogeneous tissue expression of combined respiratory chain deficiencies. *Virchows Archiv A* **419**, 355-362, doi:10.1007/bf01606527 (1991).
- 52 Witt, C. *et al.* Respiratory muscle weakness and normal ventilatory drive in dilative cardiomyopathy. *European heart journal* **18**, 1322-1328 (1997).
- 53 Lecarpentier, Y. *et al.* Mechanics, energetics, and crossbridge kinetics of rabbit diaphragm during congestive heart failure. *The FASEB Journal* **12**, 981-989 (1998).
- 54 van Hees, H. W. H. *et al.* Impaired isotonic contractility and structural abnormalities in the diaphragm of congestive heart failure rats. *International Journal of Cardiology* **128**, 326-335, doi:<http://dx.doi.org/10.1016/j.ijcard.2007.06.080> (2008).
- 55 Hammond, M. D., Bauer, K. A., Sharp, J. T. & Rocha, R. D. Respiratory muscle strength in congestive heart failure. *Chest* **98**, 1091-1094 (1990).
- 56 Coirault, C. *et al.* Oxidative stress of myosin contributes to skeletal muscle dysfunction in rats with chronic heart failure. *American Journal of Physiology-Heart and Circulatory Physiology* **292**, H1009-H1017 (2007).
- 57 Lecarpentier, Y. *et al.* Impaired load dependence of diaphragm relaxation during congestive heart failure in the rabbit. *Journal of applied physiology (Bethesda, Md. : 1985)* **87**, 1339-1345 (1999).
- 58 Lecarpentier, Y. *et al.* Intrinsic alterations of diaphragm muscle in experimental cardiomyopathy. *American heart journal* **126**, 770-776 (1993).
- 59 Lima, A. R. R. *et al.* Heart failure-induced diaphragm myopathy. *Cellular Physiology and Biochemistry* **34**, 333-345, doi:10.1159/000363003 (2014).
- 60 Mancini, D. M., Henson, D., Lamanca, J. & Levine, S. Evidence of reduced respiratory muscle endurance in patients with heart failure. *Journal of the American College of Cardiology* **24**, 972-981, doi:[http://dx.doi.org/10.1016/0735-1097\(94\)90858-3](http://dx.doi.org/10.1016/0735-1097(94)90858-3) (1994).
- 61 Huxley, A. F. & Simmons, R. M. Proposed mechanism of force generation in striated muscle. *Nature* **233**, 533-538 (1971).

- 62 Huxley, H. The crossbridge mechanism of muscular contraction and its implications. *Journal of experimental biology* **115**, 17-30 (1985).
- 63 Bagni, M., Cecchi, G. & Schoenberg, M. A model of force production that explains the lag between crossbridge attachment and force after electrical stimulation of striated muscle fibers. *Biophysical Journal* **54**, 1105 (1988).
- 64 Roots, H., Offer, G. & Ranatunga, K. Comparison of the tension responses to ramp shortening and lengthening in intact mammalian muscle fibres: crossbridge and non-crossbridge contributions. *Journal of muscle research and cell motility* **28**, 123-139 (2007).
- 65 Pate, E. & Cooke, R. A model of crossbridge action: the effects of ATP, ADP and Pi. *J.Muscle Res.Cell Motil.* **10**, 181-196 (1989).
- 66 Sweeney, H. L. & Houdusse, A. The motor mechanism of myosin V: insights for muscle contraction. *Philosophical Transactions of the Royal Society-Ser B-Biological Sciences* **359**, 1829-1842 (2004).
- 67 Gordon, A. M., Huxley, A. F. & Julian, F. J. The variation in isometric tension with sarcomere length in vertebrate muscle fibres. *J.Physiol* **184**, 170-192 (1966).
- 68 Granzier, H. L. & Pollack, G. H. The descending limb of the force-sarcomere length relation of the frog revisited. *J.Physiol* **421**, 595-615 (1990).
- 69 Allinger, T. L., Herzog, W. & Epstein, M. Force-length properties in stable skeletal muscle fibers--theoretical considerations. *J.Biomech.* **29**, 1235-1240 (1996).
- 70 Gordon, A., Homsher, E. & Regnier, M. Regulation of contraction in striated muscle. *Physiological reviews* **80**, 853-924 (2000).
- 71 Brenner, B. & Eisenberg, E. Rate of force generation in muscle: correlation with actomyosin ATPase activity in solution. *Proceedings of the National Academy of Sciences* **83**, 3542-3546 (1986).
- 72 Edman, K. in *Muscle Biophysics* 7-40 (Springer, 2010).

- 73 Hill, A. V. & Howarth, J. V. The Reversal of Chemical Reactions in Contracting Muscle during an Applied Stretch. *Proceedings of the Royal Society of London B: Biological Sciences* **151**, 169-193 (1959).
- 74 Bárány, M. ATPase activity of myosin correlated with speed of muscle shortening. *The Journal of general physiology* **50**, 197-218 (1967).
- 75 Edman, K., Månsson, A. & Caputo, C. The Biphasic Force–Velocity Relationship in Frog Muscle Fibres and its Evaluation in Terms of Cross-Bridge Function. *The Journal of physiology* **503**, 141-156 (1997).
- 76 Bickham, D. C. *et al.* Millisecond-scale biochemical response to change in strain. *Biophysical Journal* **101**, 2445-2454 (2011).
- 77 Linari, M., Woledge, R. & Curtin, N. Energy storage during stretch of active single fibres from frog skeletal muscle. *The Journal of physiology* **548**, 461-474 (2003).
- 78 Bagni, M. A., Cecchi, G., Colombini, B. & Colomo, F. A non-cross-bridge stiffness in activated frog muscle fibers. *Biophysical Journal* **82**, 3118-3127 (2002).
- 79 Nocella, M., Colombini, B., Bagni, M. A., Bruton, J. & Cecchi, G. Non-crossbridge calcium-dependent stiffness in slow and fast skeletal fibres from mouse muscle. *J Muscle Res Cell Motil* **32**, 403-409, doi:10.1007/s10974-011-9274-5 (2012).
- 80 Joumaa, V., Rassier, D. E., Leonard, T. R. & Herzog, W. The origin of passive force enhancement in skeletal muscle. *American Journal of Physiology - Cell Physiology* **294**, C74-C78 (2008).
- 81 Piazzesi, G. *et al.* Skeletal muscle performance determined by modulation of number of myosin motors rather than motor force or stroke size. *Cell* **131**, 784-795 (2007).
- 82 Linari, M. *et al.* A combined mechanical and X-ray diffraction study of stretch potentiation in single frog muscle fibres. *The Journal of physiology* **526**, 589-596 (2000).
- 83 Bullimore, S. R., Leonard, T. R., Rassier, D. E. & Herzog, W. History-dependence of isometric muscle force: effect of prior stretch or shortening amplitude. *Journal of biomechanics* **40**, 1518-1524, doi:10.1016/j.jbiomech.2006.06.014 (2007).

- 84 Minozzo, F. C. & Rassier, D. E. The effects of Ca²⁺ and MgADP on force development during and after muscle length changes. *PloS one* **8**, e68866, doi:10.1371/journal.pone.0068866 (2013).
- 85 Herzog, W., Schachar, R. & Leonard, T. R. Characterization of the passive component of force enhancement following active stretching of skeletal muscle. *The Journal of experimental biology* **206**, 3635-3643 (2003).
- 86 Herzog, W. & Leonard, T. R. The role of passive structures in force enhancement of skeletal muscles following active stretch. *Journal of biomechanics* **38**, 409-415, doi:10.1016/j.jbiomech.2004.05.001 (2005).
- 87 Minozzo, F. C., Baroni, B. M., Correa, J. A., Vaz, M. A. & Rassier, D. E. Force produced after stretch in sarcomeres and half-sarcomeres isolated from skeletal muscles. *Scientific reports* **3**, 2320, doi:10.1038/srep02320 (2013).
- 88 Minozzo, F. C., Hilbert, L. & Rassier, D. E. Pre-power-stroke cross-bridges contribute to force transients during imposed shortening in isolated muscle fibers. *PloS one* **7**, e29356, doi:10.1371/journal.pone.0029356 (2012).
- 89 Rassier, D. E. The mechanisms of the residual force enhancement after stretch of skeletal muscle: non-uniformity in half-sarcomeres and stiffness of titin. *Proceedings. Biological sciences / The Royal Society* **279**, 2705-2713, doi:10.1098/rspb.2012.0467 (2012).
- 90 Leonard, T. R. & Herzog, W. Regulation of muscle force in the absence of actin-myosin-based cross-bridge interaction. *American Journal of Physiology - Cell Physiology* **299**, C14-C20 (2010).
- 91 Rassier, D. E. & Pavlov, I. Force produced by isolated sarcomeres and half-sarcomeres after an imposed stretch. *American Journal of Physiology - Cell Physiology* **302**, C240-C248, doi:10.1152/ajpcell.00208.2011 (2012).
- 92 Rassier, D. E. Molecular basis of force development by skeletal muscles during and after stretch. *Molecular & cellular biomechanics : MCB* **6**, 229-241 (2009).

- 93 Edman, K. A. P. & Reggiani, C. Redistribution of sarcomere length during isometric contraction of frog muscle fibres and its relation to tension creep. *Journal of Physiology* **351**, 169-198 (1984).
- 94 Julian, F. J. & Morgan, D. L. The effect on tension of non-uniform distribution of length changes applied to frog muscle fibres. *Journal of Physiology* **293**, 379-392 (1979).
- 95 Pun, C., Syed, A. & Rassier, D. E. History-dependent properties of skeletal muscle myofibrils contracting along the ascending limb of the force-length relationship. *Proceedings of the Royal Society B: Biological Sciences* **277**, 475-484 (2010).
- 96 Rassier, D. E., Herzog, W. & Pollack, G. H. Dynamics of individual sarcomeres during and after stretch in activated single myofibrils. *Proceedings of the Royal Society B: Biological Sciences* **270**, 1735-1740 (2003).
- 97 Getz, E. B., Cooke, R. & Lehman, S. L. Phase transition in force during ramp stretches of skeletal muscle. *Biophysical Journal* **75**, 2971-2983 (1998).
- 98 Minozzo, F. C. & Rassier, D. E. Effects of blebbistatin and Ca²⁺ concentration on force produced during stretch of skeletal muscle fibers. *Am J Physiol Cell Physiol* **299**, C1127-1135, doi:10.1152/ajpcell.00073.2010 (2010).
- 99 Ranatunga, K. W., Roots, H., Pinniger, G. J. & Offer, G. W. Crossbridge and non-crossbridge contributions to force in shortening and lengthening muscle. **682**, 207-221 (2010).
- 100 Pinniger, G. J., Ranatunga, K. W. & Offer, G. W. Crossbridge and non-crossbridge contributions to tension in lengthening rat muscle: Force-induced reversal of the power stroke. *Journal of Physiology* **573**, 627-643 (2006).
- 101 Cornachione, A. S. & Rassier, D. E. A non-cross-bridge, static tension is present in permeabilized skeletal muscle fibers after active force inhibition or actin extraction. *Am J Physiol Cell Physiol* **302**, C566-574, doi:10.1152/ajpcell.00355.2011 (2012).
- 102 Granzier, H. L. & Labeit, S. The giant muscle protein titin is an adjustable molecular spring. *Exercise and sport sciences reviews* **34**, 50-53 (2006).

- 103 Labeit, D. *et al.* Calcium-dependent molecular spring elements in the giant protein titin. *Proceedings of the National Academy of Sciences* **100**, 13716-13721, doi:10.1073/pnas.2235652100 (2003).
- 104 Rassier, D. E., Lee, E.-J. & Herzog, W. Modulation of passive force in single skeletal muscle fibres. *Biology Letters* **1**, 342-345 (2005).
- 105 Begay, R. L. *et al.* Role of Titin Missense Variants in Dilated Cardiomyopathy. *Journal of the American Heart Association* **4**, doi:10.1161/jaha.115.002645 (2015).
- 106 Campuzano, O. *et al.* Rare Titin (TTN) Variants in Diseases Associated with Sudden Cardiac Death. *International journal of molecular sciences* **16**, 25773-25787, doi:10.3390/ijms161025773 (2015).
- 107 Franssen, C. & Gonzalez Miqueo, A. The role of titin and extracellular matrix remodelling in heart failure with preserved ejection fraction. *Netherlands heart journal : monthly journal of the Netherlands Society of Cardiology and the Netherlands Heart Foundation* **24**, 259-267, doi:10.1007/s12471-016-0812-z (2016).
- 108 Gerull, B. The Rapidly Evolving Role of Titin in Cardiac Physiology and Cardiomyopathy. *The Canadian journal of cardiology* **31**, 1351-1359, doi:10.1016/j.cjca.2015.08.016 (2015).
- 109 Zhou, Q. *et al.* Pressure Overload by Transverse Aortic Constriction Induces Maladaptive Hypertrophy in a Titin-Truncated Mouse Model. *BioMed research international* **2015**, 163564, doi:10.1155/2015/163564 (2015).
- 110 Spudich, James A. Hypertrophic and Dilated Cardiomyopathy: Four Decades of Basic Research on Muscle Lead to Potential Therapeutic Approaches to These Devastating Genetic Diseases. *Biophysical Journal* **106**, 1236-1249, doi:<http://dx.doi.org/10.1016/j.bpj.2014.02.011> (2014).
- 111 Stassijns, G. *et al.* Effects of dilated cardiomyopathy on the diaphragm in the Syrian hamster. *The European respiratory journal* **13**, 391-397 (1999).

- 112 MacFarlane, N. G., Darnley, G. M. & Smith, G. L. Cellular basis for contractile dysfunction in the diaphragm from a rabbit infarct model of heart failure. *Am J Physiol Cell Physiol* **278**, C739-746 (2000).
- 113 Lunde, P. K. *et al.* Contraction and intracellular Ca²⁺ handling in isolated skeletal muscle of rats with congestive heart failure. *Circulation research* **88**, 1299-1305 (2001).
- 114 Hershberger, R. E., Hedges, D. J. & Morales, A. Dilated cardiomyopathy: the complexity of a diverse genetic architecture. *Nature reviews. Cardiology* **10**, 531-547, doi:10.1038/nrcardio.2013.105 (2013).
- 115 McNally, E. M., Golbus, J. R. & Puckelwartz, M. J. Genetic mutations and mechanisms in dilated cardiomyopathy. *The Journal of clinical investigation* **123**, 19-26, doi:10.1172/jci62862 (2013).
- 116 Seidman, J. G. & Seidman, C. The Genetic Basis for Cardiomyopathy: from Mutation Identification to Mechanistic Paradigms. *Cell* **104**, 557-567, doi:[http://dx.doi.org/10.1016/S0092-8674\(01\)00242-2](http://dx.doi.org/10.1016/S0092-8674(01)00242-2) (2001).
- 117 Palmer, B. M. *et al.* Differential cross-bridge kinetics of FHC myosin mutations R403Q and R453C in heterozygous mouse myocardium. *American journal of physiology. Heart and circulatory physiology* **287**, H91-99, doi:10.1152/ajpheart.01015.2003 (2004).
- 118 Palmer, B. M. *et al.* Myofilament mechanical performance is enhanced by R403Q myosin in mouse myocardium independent of sex. *American journal of physiology. Heart and circulatory physiology* **294**, H1939-1947, doi:10.1152/ajpheart.00644.2007 (2008).
- 119 Tyska, M. *et al.* Single-molecule mechanics of R403Q cardiac myosin isolated from the mouse model of familial hypertrophic cardiomyopathy. *Circulation research* **86**, 737-744 (2000).
- 120 Geisterfer-Lowrance, A. A., Christe, M., Conner, D. A. & Ingwall, J. S. A mouse model of familial hypertrophic cardiomyopathy. *Science* **272**, 731 (1996).
- 121 Malmqvist, U. P., Aronshtam, A. & Lowey, S. Cardiac myosin isoforms from different species have unique enzymatic and mechanical properties. *Biochemistry* **43**, 15058-15065, doi:10.1021/bi0495329 (2004).

- 122 Geiger, P. C., Cody, M. J. & Sieck, G. C. *Force-calcium relationship depends on myosin heavy chain and troponin isoforms in rat diaphragm muscle fibers*. Vol. 87 (1999).
- 123 Marian, A. J. *et al.* A transgenic rabbit model for human hypertrophic cardiomyopathy. *Journal of Clinical Investigation* **104**, 1683-1692 (1999).
- 124 Sanbe, A. *et al.* Transgenic Rabbit Model for Human Troponin I-Based Hypertrophic Cardiomyopathy. *Circulation* **111**, 2330-2338 (2005).
- 125 Fabiato, A. Computer programs for calculating total from specified free or free from specified total ionic concentrations in aqueous solutions containing multiple metals and ligands. *Methods in enzymology* **157**, 378-417 (1988).
- 126 Tatsumi, R., Sheehan, S., Iwasaki, H., Hattori, A. & Allen, R. E. Mechanical stretch induces activation of skeletal muscle satellite cells in vitro. *Experimental cell research* **267**, 107-114 (2001).
- 127 Lamont, P. J. *et al.* Novel mutations widen the phenotypic spectrum of slow skeletal/beta-cardiac myosin (MYH7) distal myopathy. *Human mutation* **35**, 868-879, doi:10.1002/humu.22553 (2014).
- 128 Fananapazir, L., Dalakas, M. C., Cyran, F., Cohn, G. & Epstein, N. D. Missense mutations in the beta-myosin heavy-chain gene cause central core disease in hypertrophic cardiomyopathy. *Proceedings of the National Academy of Sciences of the United States of America* **90**, 3993-3997 (1993).